

A Comprehensive Ongoing Survey of the Near-Earth Asteroid Population for Human Mission Accessibility

Brent W. Barbee*, Timothy Esposito†, Elfego Piñon III‡, Sun Hur-Diaz§
Emergent Space Technologies, Inc., Greenbelt, MD, 20770-6334, USA

Ronald G. Mink¶
NASA Goddard Space Flight Center, Greenbelt, MD, 20771, USA

Daniel R. Adamo||
Houston, TX, 77059, USA

There are currently 7069 known Near-Earth Asteroids (NEAs) and more are being discovered on a continual basis; it is likely that the total NEA population consists of at least hundreds of thousands of objects. NEAs have orbits that bring them into close proximity with Earth's orbit, making them both a unique hazard to life on Earth and a unique opportunity for science and exploration. The current presidential administration has proposed that NASA send humans to an asteroid by the mid-2020s as part of the Flexible Path architecture. A study was therefore undertaken to identify NEAs that are accessible for round-trip human missions using a heavy-lift launch architecture. A fully parametrized, highly efficient algorithm was developed to accomplish this, allowing changes in vehicle parameters to be studied and enabling the accessibility analysis to keep pace with the NEA discovery rate, which is increasing as new telescopes, such as Pan-STARRS, become active. To date, the accessibility analysis algorithm has identified 59 accessible NEAs and 10 marginally inaccessible NEAs. Of the 59 accessible NEAs, 14 offer attractive mission opportunities between 2016 and 2030, with round-trip flight times between 54 and 192 days. Some example opportunities for robotic science/reconnaissance precursor missions and sample return missions to these accessible NEAs have also been computed.

I. Introduction

NEAR-Earth Objects (NEOs) are asteroids and comets whose heliocentric orbits bring them close to Earth's orbit. Currently, the number of known Near-Earth Asteroids (NEAs) greatly exceeds the number of known Near-Earth Comets (NECs). NEAs offer a wide variety of interesting destinations for science and exploration, though the close proximity of their orbits to Earth's orbit also makes NEAs a potential threat to life on Earth. A number of robotic science missions have been deployed to asteroids and comets, and more such missions are being planned.

We do not currently know how many NEAs exist, but thousands of them have been discovered and statistical models of the NEA population suggest that there may be hundreds of thousands or even millions of these objects, with sizes ranging from several meters to several kilometers or more. NEO search programs began in the 1990s and today there are multiple observatories scanning the skies for NEOs. Current and past survey systems include Lincoln Near-Earth Asteroid Research (LINEAR) (1997-Present), Near Earth

*Aerospace Engineer, 6301 Ivy Lane, Suite 720, brent.barbee@emergentspace.com, AIAA Member.

†Director, Mission Operations Technologies, timothy.esposito@emergentspace.com, AIAA Member.

‡Senior GN&C Engineer, elfego.pinon@emergentspace.com, AIAA Member.

§Vice President, sun.hur-diaz@emergentspace.com, AIAA Senior Member.

¶Systems Engineer, Code 592, 8800 Greenbelt Road, ronald.g.mink@nasa.gov.

||Astrodynamics Consultant, 4203 Moonlight Shadow Ct., adamod@earthlink.net, AIAA Senior Member.

Asteroid Tracking (NEAT) (1995-2007), Spacewatch (1989-Present), Lowell Observatory Near-Earth-Object Search (LONEOS) (1993-2008), and the Catalina Sky Survey (1998-Present). Additionally, there is the Wide-Field Infrared Survey Explorer (WISE), a NASA-funded infrared space telescope that launched on December 14th, 2009, and has discovered 94 NEAs and 15 comets as of July 14th, 2010^a. One of the key advantages of WISE is that it is capable of discovering asteroids (and measuring their diameters) by sensing their infrared signatures^b; this allows WISE to detect asteroids that reflect little visible light and are thus extremely difficult to detect from the ground, where infrared observations are masked by atmospheric moisture. As of July 14th, 2010, a total of 7069 NEAs^c have been discovered, and more are being found on a continual basis.

The annual NEA discovery rate has been increasing and will continue to increase as new observing assets become available. The Panoramic Survey Telescope and Rapid Response System (Pan-STARRS) is a telescope array and computing facility that will perform continuous surveys of the sky and discover many new objects, including NEAs. The first Pan-STARRS telescope went online on December 6th, 2008, and full time science operations began on May 13th, 2010; the system will ultimately consist of four telescopes. The Large Synoptic Survey Telescope (LSST) is a wide-field survey reflecting telescope that should begin construction in 2010 and become operational in 2015. Both Pan-STARRS and LSST are expected to discover large numbers of NEAs.

In this paper we will present the methodology that we have developed to survey this diverse and growing population of known NEAs in an ongoing search for those that are accessible for human exploration.

I.A. Motivation

There are a variety of compelling reasons to study NEAs and send both robots and astronauts to visit them. They are vital targets for fundamental solar system science and the collision threat they pose to life on Earth makes it even more imperative that we understand their sizes, compositions, internal structures, spin states, and orbits, among other characteristics, so that we may be prepared to act when a NEA on a collision course with Earth is discovered. The close proximity of NEA orbits to Earth's orbit also raises the possibility of short duration round-trip missions to them, which would allow us to send humans to visit NEAs. Indeed, finding NEAs for which such missions may be possible is the primary objective of the research presented herein.

I.A.1. Solar System Science

Asteroids and comets are largely unchanged in composition since the early days of our solar system, and studying them provides vital insight into our origins. For instance, the Stardust mission to the comet Wild 2 returned samples of cometary material that proved the existence of large-scale circulation patterns in the solar nebula, which completely revised our views of nebular dynamics and chemistry.¹ Additionally, it is possible that asteroids and comets may have delivered vast quantities of water^d to the young Earth and may have also have carried the seeds of life itself^e. Another tantalizing possibility is that besides learning about our own solar system, we can apply this knowledge to understand other star systems and the potential for life elsewhere in the universe.

I.A.2. The Impact Hazard and Planetary Defense

NEAs also pose a hazard to Earth as they can collide with our planet, sometimes to devastating effect. As of July 14th, 2010, 1139 NEAs^f were classified as Potentially Hazardous Asteroids (PHAs). PHAs are asteroids that have a Minimum Orbit Intersection Distance (MOID) with Earth less than or equal to 0.05 AU and an absolute magnitude^g, H , of 22.0 or brighter ($H \leq 22.0$), which corresponds to a minimum size^h

^a<http://neo.jpl.nasa.gov/stats/wise/>

^b<http://wise.ssl.berkeley.edu/science.html>

^c<http://neo.jpl.nasa.gov/stats/>

^d<http://www.cosmosmagazine.com/news/3427/ice-asteroids-likely-source-earths-water>

^e<http://www.cosmosmagazine.com/news/3441/carbon-rich-comet-fragments-found-antarctic-snow>

^f<http://neo.jpl.nasa.gov/neo/groups.html>

^gAbsolute magnitude (for Solar System bodies) is defined as the apparent magnitude of an object if it were 1 AU from the Sun and the observer, and at a phase angle of zero degrees.

^h $H = 22.0$ generally corresponds to a size range of 110–240 m, but for the purposes of defining PHAs an albedo of 13% is also assumed, in which case $H = 22.0$ then corresponds to a size of 150 m.

of approximately 150 m.

Earth is struck by very small NEAs on a regular basis, and flybys by NEAs within the Moon's orbit occur every few weeks. The surface of our moon is clearly covered in craters from past impacts and our own planet also bears the scars of bombardment, though they are largely obscured by weathering, vegetation, and the fact that the majority of Earth's surface is covered by water. Nevertheless, at the time of this writing there are 176 confirmed impact structures on Earthⁱ, many of which are larger than 20 km in diameter. One study of the biodiversity reflected in the fossil record has indicated that there is a periodicity to mass extinctions,² and while a direct cause has not been identified for many extinction events, we do know that the impact that created the famous Chicxulub crater in the Yucatan peninsula approximately 65 million years ago did cause the Cretaceous-Paleogene (K-Pg) extinction event^j, during which the dinosaurs were made extinct, along with most other species living at the time.³ The NEO that caused the (K-Pg) boundary extinction event is estimated to have been between 9 and 19 km in diameter, but the more numerous smaller NEOs can still cause considerable damage. Impacts by NEOs that are one to several km in diameter can cause extinction-level events, while NEOs that are on the order of several hundred meters in diameter can devastate entire nations or regions. Even small NEOs that are on the order of tens of meters in size can devastate entire cities. For example, during the Tunguska event, which occurred in Siberia in the year 1908, a small NEO estimated to have been between 10 to 20 m in size exploded several kilometers above the ground and devastated an area the size of Washington, DC.

While our own planet and moon show ample evidence of past impact events, we have observed three large-scale collisions of comets and asteroids with the planet Jupiter. Between July 16th and 22nd in 1994, more than 20 pieces of the comet Shoemaker-Levy 9 struck Jupiter, and our observations of that event constituted the first time we had ever directly observed such a collision. Since then Jupiter has been hit twice more that we are aware of: on July 19th, 2009, and June 3rd, 2010.

Impacts by NEAs are random, aperiodic events and can occur at any time with little or no warning. Our detection and characterization methods are improving (and must continue to improve), giving us the chance to have some advance warning, but NEA deflection systems have yet to be built and tested. Our current and near-term technology may offer the tools with which to prevent NEA impacts but we must develop and test the various proposed NEA deflection systems before they can be relied upon; this includes developing a proficiency with proximity operations in the vicinity of NEAs, which possess highly irregular, albeit weak, gravitational fields that have challenged the guidance and control systems of robotic spacecraft. We must also discover and characterize NEAs to inform deflection system design and deployment; it is serendipitous that discovery and characterization efforts simultaneously serve the purposes of fundamental science, human exploration, and planetary defense against NEA impacts.⁴

I.A.3. Resource Utilization

Besides being scientifically interesting and posing a threat, NEAs contain a variety of raw materials that could be harvested. NEAs contain useful substances such as iron, rock, water, carbon, nitrogen, semiconductor and platinum group metals, and trapped gasses such as carbon dioxide and ammonia^k. These resources can be utilized for a variety of purposes, including the manufacture of radiation shielding and spacecraft propellant, without needing to expend the tremendous energy required to launch the raw materials into space from Earth. Harnessing these resources will of course require extensive infrastructure development and a greatly scaled-up space economy. However, the first important step is to discover, explore, and study NEAs so that we can survey the population, identify the available resources, and develop appropriate utilization plans. Doing so will clearly require rigorous scientific study, the ability to operate in the vicinity of NEAs and on their surfaces, and the ability to modify their orbits. Thus the goal of NEA resource utilization is clearly synergistic with the goals of solar system science, planetary defense, and human exploration.

I.A.4. Human Exploration

While the orbital proximity of NEAs makes them a hazard to Earth, it also offers a unique opportunity since many may be accessible for human missions with very short round-trip flight times, assuming the existence

ⁱ<http://www.unb.ca/passc/ImpactDatabase/index.html> - An interactive map showing the locations and characteristics of the impact structures can be found here: <http://impact.scaredycatfilms.com/>

^jIn the past this event was commonly referred to as the Cretaceous/Tertiary (K/T) boundary extinction event.

^khttp://www.space.com/adastra/060209_adastra_mining.html

of an adequate crew vehicle and heavy-lift launch capability. Human missions to NEAs would further our crucial scientific study of asteroids and simultaneously provide us with much-needed experience in true interplanetary travel prior to larger, longer-duration expeditions to more distant destinations, such as Mars. Perhaps most importantly, a human mission to an NEA would be the most ambitious journey of human discovery since Apollo and would serve to reinvigorate our space program and renew public passion for space exploration. In April of 2010, the President of the United States set a goal for NASA to send humans to an asteroid by the year 2025 as part of the proposed “Flexible Path” plan for human space exploration, which still needs to win Congressional approval¹.

I.B. Background

Our NEA accessibility study began in early November of 2009 and algorithm development was essentially complete by early December of 2009. The 6496 NEAs known as of November 16th, 2009 were processed in early December using the prototype processing software that had been developed up to that point, and on December 10th, 2009, the 6611 known NEAs were processed using the finalized accessibility analysis software. On February 19th, 2010, the 142 NEAs discovered since December 10th, 2009, were processed. By March 26th, 2010, the post-processing software for visualizing the NEA accessibility space was completed and the study was paused pending future funding.

The profile of a human mission to a NEA is shown in figure 1. The crew vehicle is injected by the Earth Departure Stage (EDS) of the launch vehicle onto a trajectory that will intercept the NEA. Upon arrival in the vicinity of the NEA, the crew vehicle’s primary thruster will perform a maneuver to match the NEA’s orbit a small distance from the NEA itself. This is the primary rendezvous maneuver, which will be followed by small terminal rendezvous and proximity operations maneuvers—which are beyond our scope here—that will bring the crew vehicle very close to the NEA and keep it there for a period of time (the crew vehicle may station-keep near the NEA or execute small trajectories to fly around it, etc.).

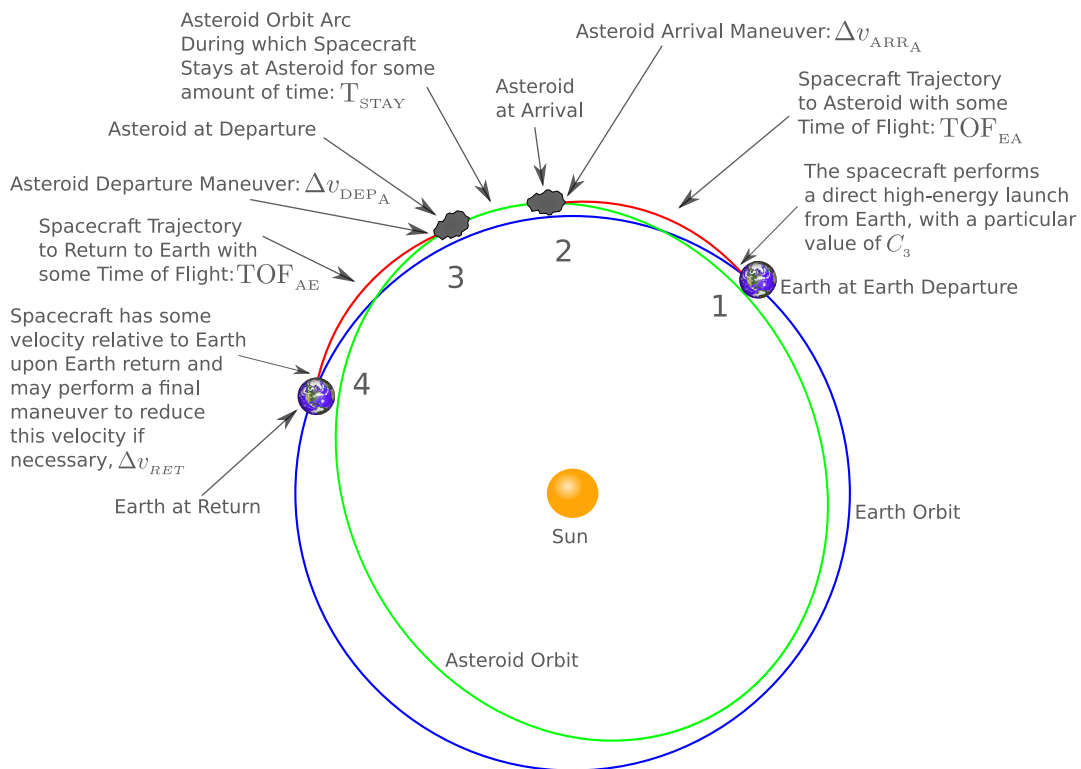


Figure 1. Mission profile.

After the designated stay time at the NEA has elapsed, the crew vehicle’s primary thruster will perform

¹<http://www.space.com/news/obama-space-plan-speech-100415.html>

a maneuver that will place it on a trajectory that will bring it back to Earth some time later. Upon Earth return, the crew vehicle will ballistically re-enter the atmosphere, similar to the procedure for lunar missions. However, if the natural velocity of the crew vehicle relative to Earth (arising from orbital mechanics) exceeds safety limits (e.g., the velocity is too high for the heat shield to tolerate), then the crew vehicle’s primary thruster may perform one final maneuver to reduce its re-entry velocity accordingly^m.

II. Methodology

Whether a particular asteroid is considered *accessible* for human exploration depends on a variety of factors. The geometry and phasing of the asteroid’s orbit relative to that of Earth must be conducive to a round-trip trajectory that consists of three phases: flight from Earth to the asteroid, some stay time at the asteroid, and flight from the asteroid back to Earth, as shown in the mission profile diagram presented in figure 1.

However, even if the relative orbit geometry and phasing seem favorable, the deciding factor that determines whether an asteroid is accessible for a round-trip human mission is ultimately the performance of both the launch vehicle and the crew vehicle; it is obvious that less capable vehicles would naturally be unable to fly round-trip missions to certain asteroids that would be reachable by more capable vehicles.

Our accessibility definition is therefore purposely made dependent on vehicle performance parameters. Thus our definition of accessibility is somewhat subjective, to the extent that the performance of future launch and crew vehicles in the mid-2020s is naturally unknown at the present time. However, we designed our accessibility analysis algorithms and software to be fully parametrized, meaning that it is trivial to alter any of the vehicle performance parameters and re-execute the processing of the NEA population. This makes our accessibility assessment extremely agile, which more than compensates for the fact that it is currently somewhat subjective. As the designs for future vehicles become more firm (and as more and more NEAs are discovered), our analysis method can easily keep pace.

We utilized the method of embedded trajectory grids to assess NEA accessibility by simultaneously computing all the possible round-trip trajectories within set bounds. The embedded trajectory grids concept is depicted in figure 2 and utilizes the parametrization of the round-trip trajectory problem shown in figure 1.

Thus our accessibility definition also naturally depends on the following factors: maximum allowable round-trip flight time, lower and upper bounds for the trajectory segment flight times, step sizes at which trajectory segment flight times are sampled, lower and upper bounds for the Earth departure date, and the step size at which Earth departure date is sampled. For example, if the maximum allowable flight time was set to 360 days, then any asteroids that might have only offered feasible trajectory solutions with total round-trip flight times greater than 360 days would not have been identified as accessible. Likewise, if the lower and upper bounds on Earth departure year were set to 2016 and 2050, respectively, then if an asteroid only offers a feasible trajectory solution in a year earlier than 2016 or later than 2050, it would not have been identified as accessible. Or, if the trajectory grid sizes were too coarse, an asteroid’s feasible trajectory solutions could conceivably have been aliased out and the asteroid would have erroneously been found to be inaccessible.

We chose 360 days as the maximum round-trip flight time so that we could compare our results to those obtained from a similar study that was underway at the Jet Propulsion Laboratories (JPL) and the NASA Johnson Space Center (JSC).⁵ We chose the lower and upper bounds for Earth departure year to be 2016 and 2050, inclusive, for the same reason. Of course, more study is necessary to ascertain whether 360 days is feasible or desirable for a human interplanetary mission. Also, the currently desired time frame for Earth departure is the mid-2020s; 2016-2050 clearly includes that, but our space program certainly will not be ready to launch a human mission to an asteroid in 2016 and is currently uninterested in mission opportunities so far in the future as 2050.

We also spent time tuning the trajectory grid sizing parameters before processing the entire NEA population in order to be reasonably certain that we would not inadvertently alias out any important trajectory solutions for any of the asteroids, while at the same time making the grid sizing parameters large enough to keep the processing time manageable. We validated our choices for grid sizing parameters after initial processing was completed by re-executing the processing on the accessible and marginally inaccessible NEAs,

^mAlternatively, the re-entry speed could be reduced by extending the time interval from NEA departure to Earth return, provided that this does not lead to the violation of a maximum round-trip mission time constraint. This option has not yet been explored in our study but may be considered in future work.

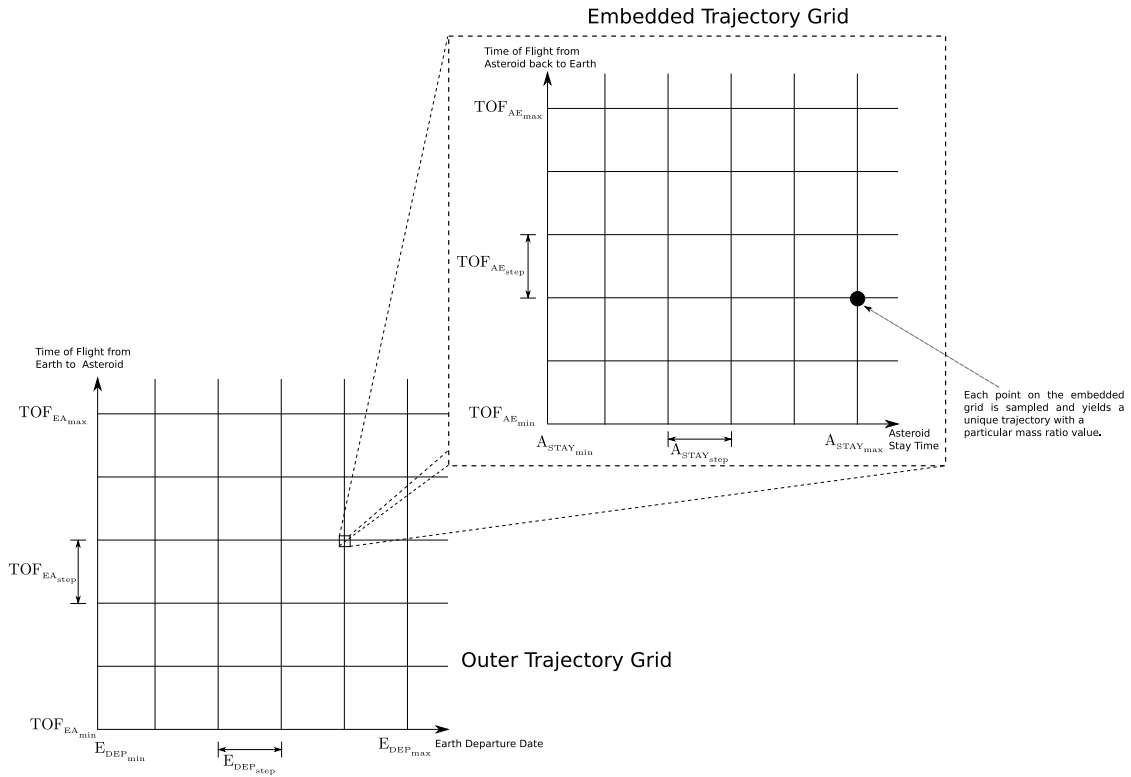


Figure 2. Embedded trajectory grids.

but using much finer grid size parameters; the results were virtually identical.

II.A. Vehicle Data

The launch vehicle performance is simply characterized by the amount of mass it can launch to high-energy direct Earth departure trajectories. The crew vehicle performance is parametrized by the following quantities: dry mass, main thruster specific impulse, and maximum atmospheric re-entry velocity. The performance values we assumed in our study for both the launch and crew vehicle are discussed in turn.

II.A.1. Launch Vehicle

We parametrize the launch vehicle performance by the curve that describes its launch mass capability as a function of the C_3 value associated with the Earth departure trajectory onto which the launch vehicle's upper stage (the Earth Departure Stage (EDS)) must place the crew vehicle. C_3 is sometimes referred to as the launch energy and serves to parametrize the amount of energy that the launch vehicle (and EDS) must be capable of imparting to the spacecraft.

In our study we utilized the launch mass vs. C_3 curve for the notional Ares V heavy-lift launch vehicle⁶ by manually tabulating data points from a plot graphic and then applying a polynomial curve fit, as shown in figure 3, which allows us to easily compute the available launch mass for any value of C_3 .

Given the political uncertainty surrounding the Constellation program and the notional nature of the Ares V design, we shall simply assume that this Ares V performance curve is representative of a future heavy-lift human-rated launch vehicle that will be available by the mid-2020s. It is also important to note that in our study we have assumed a single Ares V launch, as this was a constraint imposed by the Augustine commission. However, the current restructuring of NASA's human space flight program means that this constraint no longer applies and raises the possibility of changing the concept of operations to include multiple heavy-lift launches for human missions to a NEA. If this indeed becomes the favored mission mode we will incorporate it into our analysis methodology accordingly.

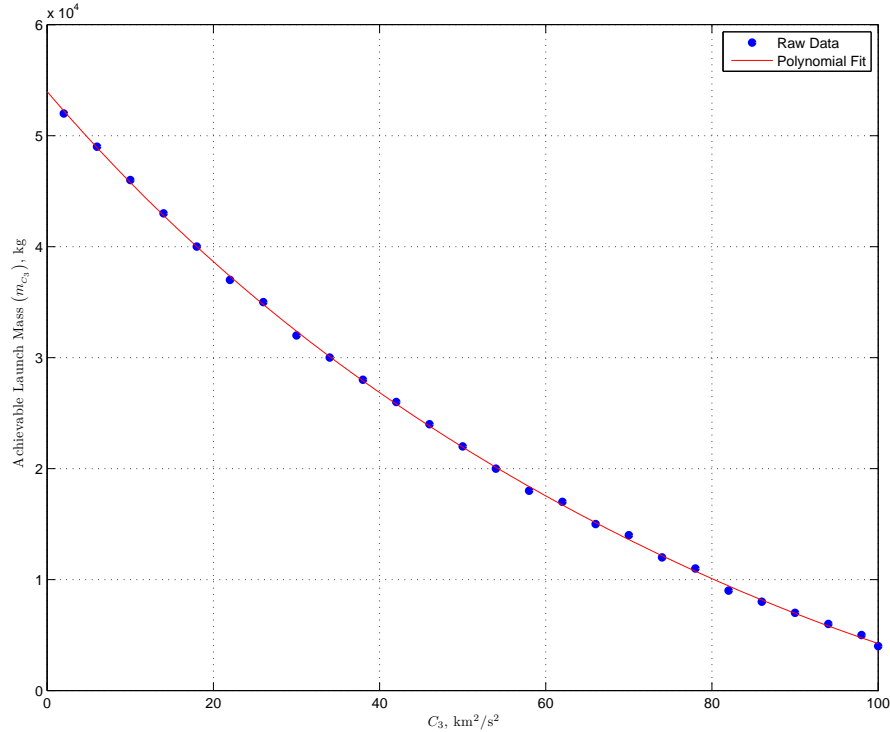


Figure 3. Notional Ares V launch mass performance as a function of C_3 .

II.A.2. Crew Vehicle Overview

We parametrize the crew vehicle performance with three parameters: the vehicle dry mass, the vehicle thruster specific impulse, and the maximum Earth atmosphere re-entry velocity that the vehicle can safely withstand (which we assume is chiefly a function of the vehicle’s heat shield).

In our study we used the notional design parameters for the Orion crew vehicle⁷ as it represents the most recent and rigorous design we are aware of for a vehicle capable of carrying crew on a mission beyond Low Earth Orbit (LEO). However, with the current political uncertainty surrounding the Constellation program, the fact that the design parameters are only notional (regardless of the political situation), and the fact that Orion was designed for lunar missions—not asteroid missions—we recognize that these values may only be treated as reasonably representative. While we cannot speculate as to what sort of crew vehicle technology might actually be available by the mid-2020s, it is reasonable to assume that a future crew vehicle’s performance parameters might resemble those of the current notional Orion design. No more credible source of future crew vehicle performance data exists (of which we are aware), in any case. In fact, we have noted the lack of any truly rigorous study as to just what the requirements ought to be for a crew vehicle capable of asteroid missions, and we recommend such study as an important future work topic.

For the Orion crew vehicle, we have assumed a dry mass of 17,078 kg, a thruster specific impulse of 314 seconds, and a maximum Earth atmosphere re-entry velocity of 12 km/s. The dry mass and thruster specific impulse are as per the available design documentation,⁷ and the maximum re-entry velocity is an accepted value for crew vehicles returning from Mars.⁸ We believe that using this maximum re-entry velocity for our study is appropriate since NEAs are widely considered to be stepping-stones towards Mars missions.

II.A.3. Crew Vehicle Dry Mass

Here we take “dry” mass to mean the actual physical mass of the crew vehicle and all of its hardware, the crew, their consumables, some proximity operations propellant, etc. Essentially, *all* of the vehicle mass

except the propellant required to perform the primary trajectory maneuvers using the spacecraft's main orbital maneuvering thruster, which will generally be different than the smaller thrusters that are used for attitude control and proximity operations. This is a good assumption because it is conservative: as the crew vehicle expends small quantities of proximity operations and attitude control fuel, and as the crew consumes their consumables, the effective dry mass of the crew vehicle will decrease slightly, making it slightly more agile than we are considering it to be here.

In future work it would be preferable to derive a rigorous vehicle dry mass that scales appropriately with mission duration. Clearly, the number of crew members and the amount of consumables they must carry would vary with the mission duration; their expected total radiation dose would also vary with mission duration and therefore so would the amount of radiation shielding required (which of course strongly affects the vehicle dry mass). Articulating and discussing the many spacecraft design considerations for interplanetary human space flight is beyond our scope here, but we strongly recommend research in this area for future work. For now, we shall make the assumption that the notional Orion spacecraft dry mass would provide the crew adequate living volume, consumables, and radiation protection for a multi-month round-trip mission to an NEA.

II.A.4. Crew Vehicle Thruster Specific Impulse

A common storable hypergolic^a bipropellant consists of the fuel, monomethyl hydrazine ((CH₃)NH(NH₂)), and oxidizer, nitrogen tetroxide (N₂O₄), which together provide a theoretical specific impulse of 342 seconds in vacuum.⁹ However, this specific impulse rating assumes perfect chemical equilibrium at each stage of the expansion,⁹ and so an achievable specific impulse of 314 seconds is reasonable.

For future work we have considered the possibility of varying the crew vehicle thruster specific impulse and re-executing the accessibility analysis to see what effect this has on the NEA accessibility space; we would expect the accessibility space to expand with a more capable crew vehicle thruster. In particular, marginally inaccessible NEAs might become accessible, or previously accessible NEAs might become reachable with shorter round-trip flight times since the crew vehicle ΔV capability would increase (all else being equal), permitting more energetic (faster) trajectory segments to be flown and extending the duration of the viable launch season.

We have identified two candidates for enhanced crew vehicle thruster specific impulse values: 365 seconds and 450 seconds. The former corresponds to the cryogenic bipropellant combination of liquid oxygen and liquid methane (LOX/LCH₄).¹⁰ The latter corresponds to the well-known combination of liquid oxygen and liquid hydrogen (LOX/LH₂). However, both of these propellant combinations would currently suffer from storage problems in the space environment, rendering them impractical for the purposes of a human mission to an asteroid. (It is worth noting that the storage requirements are somewhat less stringent for LOX/LCH₄ compared to LOX/LH₂.) While we cannot speculate as to whether the required technology will mature sufficiently by the mid-2020s to allow the use of one of these propellant combinations for human missions to asteroids, it is reasonable to include them in our trade space in future work so that we may articulate their impacts on the NEA accessibility space for human exploration; such trade study results may even ultimately inform vehicle design choices and the funding of their requisite technology maturation paths.

However, it may not be useful to include specific impulses beyond 450 seconds in the trade space for future work. LOX/LH₂ currently provides the highest specific impulse^o for conventional high-thrust chemical propulsion; a *practical* high-thrust chemical propulsion system capable of a larger specific impulse would certainly be revolutionary, and it does not currently seem credible to anticipate such a propulsion technology revolution. In the event that such a technology were to unexpectedly emerge, re-executing our processing of the asteroid population with an updated thruster specific impulse is a trivial matter. It is worth noting that a lithium/fluorine propellant has been test-fired and achieved a vacuum specific impulse of 542 seconds, but the formidable problems it presents in terms of extreme toxicity, extreme explosiveness (handling hazard), extreme corrosiveness, ionized exhaust (capable of communications interference), and rarity (low availability, high cost) prevent it from being flown.

^aIn a hypergolic bipropellant, the fuel and oxidizer spontaneously ignite when they come into contact.

^oA vacuum specific impulse of 464 seconds was achieved by the Pratt & Whitney RL10B-2 rocket engine, but it is currently unclear to the authors whether this is a peak performance value or if it would be appropriate to assume for the duration of a mission to an asteroid. It is not much more than the baseline of 450 seconds in any case.

II.A.5. Crew Vehicle Maximum Re-Entry Velocity

Our assumed value of 12 km/s for the maximum Earth atmosphere re-entry velocity is perhaps somewhat generous. The fastest atmospheric re-entry recorded by humans occurred during Apollo 10 and was 11.069 km/s.¹¹ Here we are assuming that future heat shield technology will allow a re-entry velocity of 12 km/s to be safely tolerated. We are currently unaware of the maximum re-entry velocity that Apollo 10 *could* have safely tolerated (it might be higher than the 11.069 km/s experienced during the mission), so it could be that heritage heat shield technology was already able to accommodate 12 km/s or close to it; if that turns out to be the case, then 12 km/s might be less of a generous assumption than we currently believe it to be. In any case, we believe it to be a sensible assumption to make for our initial study. We may vary this maximum atmospheric re-entry velocity down or up in ongoing studies as we learn more. Doing so will have an effect on the NEA accessibility space, though it is worth noting here that many of the NEAs currently found accessible by our study offer natural re-entry velocities that are less than 12 km/s.

II.B. Ephemeris Data

The JPL HORIZONS system provides best estimate^P ephemerides for all bodies in the solar system, including the 523,550 currently known asteroids^Q (including NEAs). While planetary ephemerides are available within standard published JPL ephemeris data sets, such as the DE406, ephemeris data for comets and asteroids are only available through the HORIZONS system, which offers web, email, and telnet interfaces for accessing ephemeris data. Ephemeris data can be accessed in either ASCII text format or in SPK format for use with JPL's NAIF SPICE toolkit^F.

We decided that it would be faster to write our own code to handle the NEA ephemerides in ASCII text format rather than learn the NAIF SPICE toolkit and make our software utilize it. Furthermore, to acquire ephemeris data files for thousands of NEAs requires an automated method of access, and custom code was going to be written to accomplish that anyhow.

Our solution was to first write a Perl program capable of automatically downloading a specified list of NEA ephemeris files from the HORIZONS system via its telnet interface. These files are in ASCII text format and contain a variety of data values other than the time, position, and velocity, so a small C program was written to extract just the time, position, and velocity data and write it to a new file in a simple ASCII format that is easy to parse. The Perl program handles all of this automatically for each NEA and for the Earth. The result is a collection of properly formatted ephemeris files for each NEA and the Earth, all ready to be ingested by our accessibility analysis software.

The current list of known NEAs is accessed from the NASA/JPL NEO Program website^S. The list is displayed on the website, and we then copy it into an ASCII text file and execute a Perl script on the file to re-shape the information into the proper format for ingestion by the Perl program that automatically downloads all the NEA ephemeris files from the HORIZONS system.

Next, a C function was written to locate the position and velocity data for a particular time value within the ephemeris table contained in a file. This function was utilized to quickly obtain the position and velocity of an NEA at a given epoch during trajectory processing after the NEA ephemeris file data was loaded into memory by the accessibility analysis program. We implemented a simple but fast and effective bisection method algorithm to perform the ephemeris table searches; this algorithm is generally capable of finding the correct place in the table in approximately $\log_2 n$ tries, where n is the number of entries (ephemeris data points) in the table.¹²

In future work, a bracketing algorithm might be combined with the bisection search method to exploit the fact that time is generally increasing monotonically as the ephemeris table for a given NEA is being accessed during trajectory processing. If supplied with an accurate initial guess for the location in the table (e.g., the epoch searched for when the function was last called), the combination of bracketing and bisection can be up to a factor of $\log_2 n$ faster than bisection search alone.¹²

^PGenerally, there are insufficient observations of NEAs for their HORIZONS ephemerides to approach anything like the fidelity of a JPL developmental ephemeris for planets or for other other small bodies with decades of observations.

^Q<http://ssd.jpl.nasa.gov/?horizons>

^Fhttp://ssd.jpl.nasa.gov/?ephemerides#small_bodies

^Shttp://neo.jpl.nasa.gov/cgi-bin/neo_elem

II.C. Algorithm and Software Description

The accessibility analysis software was written entirely in the C programming language and was developed in a 64-bit Linux environment. The code can be compiled on any other platform, though 64-bit Linux is the preferred choice for large-scale scientific computing. The program accepts a single input argument, which is the file name of the main ASCII input file which contains all the user-specified parameters for the accessibility analysis. Table 1 lists all of the parameters contained within the main input file, as well the numerical values (and their units) selected for this study.

Table 1. Main input file parameters.

Parameter Description	Symbol	Value	Units
Name of file containing list of asteroid ephemeris files to process	N/A	N/A	N/A
Name of Earth ephemeris file	N/A	N/A	N/A
Location where output data files will be created	N/A	N/A	N/A
Spacecraft dry mass	m_{dry}	17078.0	kg
Spacecraft thruster exhaust velocity*	gI_{sp}	3.0792881	km/s
Maximum allowable Earth return velocity for the spacecraft	$v_{\text{ret,max}}$	12.0	km/s
Maximum allowable mass ratio	$\alpha_{\text{m,max}}$	1.0	N/A
Order of launch vehicle launch mass vs. C_3 polynomial	N/A	4	N/A
First coefficient of launch vehicle launch mass vs. C_3 polynomial	p_4	0.000103762957796459	N/A
Second coefficient of launch vehicle launch mass vs. C_3 polynomial	p_3	-0.0339588316363982	N/A
Third coefficient of launch vehicle launch mass vs. C_3 polynomial	p_2	6.1452863276501	N/A
Fourth coefficient of launch vehicle launch mass vs. C_3 polynomial	p_1	-875.921415920277	N/A
Fifth coefficient of launch vehicle launch mass vs. C_3 polynomial	p_0	53962.2893920949	N/A
Minimum C_3 for which the launch vehicle performance polynomial is defined	$C_{3,\text{min}}$	0.0	km ² /s ²
Maximum C_3 for which the launch vehicle performance polynomial is defined	$C_{3,\text{max}}$	100.0	km ² /s ²
Gravitational parameter of the Sun	μ_{S}	$1.32712440018 \times 10^{11}$	km ³ /s ²
Gravitational parameter of the Earth	μ_{E}	3.986004415×10^5	km ³ /s ²
Geocentric radius of Earth's atmospheric entry interface	r_{EA}	6500.056	km
Maximum allowable total round-trip flight time	$T_{\text{tot,max}}$	360.0	days
Minimum Earth departure date [†]	$E_{\text{DEP,min}}$	57388.0	MJD
Earth departure date scan step size	$E_{\text{DEP,step}}$	6.0	days
Maximum Earth departure date [‡]	$E_{\text{DEP,max}}$	70174.0	MJD
Minimum time of flight from Earth to asteroid	$\text{TOF}_{\text{EA,min}}$	4.0	days
Step size for scanning time of flight from Earth to asteroid	$\text{TOF}_{\text{EA,step}}$	6.0	days
Maximum time of flight from Earth to asteroid	$\text{TOF}_{\text{EA,max}}$	208.0	days
Minimum stay time at the asteroid	$A_{\text{STAY,min}}$	4.0	days
Step size for scanning stay time at the asteroid	$A_{\text{STAY,step}}$	4.0	days
Maximum stay time at the asteroid	$A_{\text{STAY,max}}$	64.0	days
Minimum time of flight from asteroid to Earth return	$\text{TOF}_{\text{AE,min}}$	4.0	days
Step size for scanning time of flight from asteroid to Earth return	$\text{TOF}_{\text{AE,step}}$	6.0	days
Maximum time of flight from asteroid to Earth return	$\text{TOF}_{\text{AE,max}}$	208.0	days

* The spacecraft thruster exhaust velocity shown here is computed using $g = 9.80665 \text{ m/s}^2$ and $I_{\text{sp}} = 314 \text{ s}$.

[†] The given MJD equates to January 1st, 2016, 00:00:00.000 UTC

[‡] The given MJD equates to January 3rd, 2051, 00:00:00.000 UTC

The program first loads and parses the main input file, storing all the input values. It then validates the input parameters, ensuring that all step size values divide evenly into the spans they are associated with, ensuring that minimum span values are less than maximum span values, and ensuring that step sizes are less than spans. Next, the program loads the ephemeris files for the Earth and asteroids into memory and ensures that all spans and step sizes specified in the main input file are compatible with the spans and step sizes found within the Earth and asteroid ephemeris files. This is necessary because all the epochs associated with the trajectory grid points must be present within the ephemeris files since no interpolation or propagation is performed by the accessibility analysis program.

At this point the program is ready to begin processing each asteroid in turn. For each asteroid, the program will loop over each possible combination of Earth departure date, flight time from Earth to the asteroid, stay time at the asteroid, and flight time from the asteroid to Earth return. The program will only process combinations that satisfy the maximum total round-trip flight time constraint, such that

$$(\text{TOF}_{\text{EA}} + A_{\text{STAY}} + \text{TOF}_{\text{AE}}) \leq T_{\text{totmax}} \quad (1)$$

For each combination of Earth departure date and flight time to the asteroid, the program solves Lambert's problem to compute the trajectory from Earth to the asteroid and then calculates the C_3 for the trajectory, equal to the square of the hyperbolic excess velocity, v_∞ , with respect to Earth on the outbound hyperbola, given by

$$C_3 = v_\infty^2 = \|\vec{v}_{i_{\text{EA}}} - \vec{v}_{E_{\text{DEP}}}\|^2 \quad (2)$$

where $\vec{v}_{i_{\text{EA}}}$ is the required initial heliocentric velocity vector that the spacecraft must have in order to be on the Earth departure trajectory to the asteroid as computed by the Lambert targeting algorithm and $\vec{v}_{E_{\text{DEP}}}$ is the heliocentric velocity vector of the Earth from the JPL HORIZONS ephemeris file at the time of Earth departure. The program then checks that the computed C_3 value is within the limits specified in the input file such that

$$C_{3\text{min}} \leq C_3 \leq C_{3\text{max}} \quad (3)$$

If C_3 is within limits, the program will then compute the ΔV required to match the asteroid's orbit upon arrival (i.e., rendezvous)

$$\Delta V_{\text{ARR}_A} = \|\vec{v}_{A_{\text{ARR}}} - \vec{v}_{f_{\text{EA}}}\| \quad (4)$$

where $\vec{v}_{A_{\text{ARR}}}$ is the heliocentric velocity of the asteroid at the time of spacecraft arrival given by the JPL HORIZONS ephemeris file and $\vec{v}_{f_{\text{EA}}}$ is the heliocentric velocity of the spacecraft at the time of asteroid arrival from the Lambert targeting results.

Next, the program will solve Lambert's problem for each combination of asteroid stay time and flight time from asteroid departure to Earth return, yielding the trajectories from the asteroid back to Earth, which begin when the asteroid stay time has elapsed. From these Lambert targeting results the program can then compute the ΔV required for the spacecraft to depart the asteroid, given by

$$\Delta V_{\text{DEP}_A} = \|\vec{v}_{i_{\text{AE}}} - \vec{v}_{A_{\text{DEP}}}\| \quad (5)$$

where $\vec{v}_{i_{\text{AE}}}$ is the initial heliocentric velocity vector that the spacecraft must have at the time of asteroid departure in order to be on the trajectory that will return to Earth and $\vec{v}_{A_{\text{DEP}}}$ is the heliocentric velocity vector of the asteroid at the time of spacecraft departure given by the JPL HORIZONS ephemeris file. The program next computes the magnitude of the heliocentric velocity of the spacecraft relative to Earth at the time of Earth return, which is

$$v_{\text{HE}} = \|\vec{v}_{f_{\text{AE}}} - \vec{v}_{E_{\text{ARR}}}\| \quad (6)$$

where $\vec{v}_{f_{\text{AE}}}$ is the heliocentric velocity vector of the spacecraft at the time of Earth arrival as given by the Lambert targeting results and $\vec{v}_{E_{\text{ARR}}}$ is the heliocentric velocity vector of the Earth at the time when the spacecraft arrives, given by the JPL HORIZONS ephemeris file. The program then computes the atmospheric re-entry velocity of the spacecraft according to

$$v_{\text{ret}} = \sqrt{v_{\text{HE}}^2 + \frac{2\mu_{\text{E}}}{r_{\text{EA}}}} \quad (7)$$

where μ_{E} is the gravitational parameter of the Earth and r_{EA} is the geocentric radius of Earth's atmospheric entry interface. If this natural re-entry velocity violates the specified maximum value, i.e., $v_{\text{ret}} > v_{\text{retmax}}$, a final ΔV is computed that will reduce the spacecraft's re-entry velocity accordingly as follows

$$\Delta V_{\text{RET}} = v_{\text{ret}} - v_{\text{retmax}} \quad (8)$$

Otherwise, if the natural re-entry velocity meets the specified constraint, i.e., $v_{\text{ret}} \leq v_{\text{ret,max}}$, then no final maneuver at the time of Earth return is required and hence $\Delta V_{\text{RET}} = 0$. Note that a large maneuver cannot be performed at entry interface and must therefore be scheduled some hours beforehand. This means that the actual maneuver will generally be larger than what is computed by Eq. (8). However, during this first phase of our study we are using Eq. (8) as an approximation and will incorporate a more accurate calculation into our algorithm during future work. It is worth noting that the majority of accessible NEAs have been found to naturally have re-entry velocities < 12 km/s and thus don't require ΔV_{RET} .

At this point all the maneuvers required of the spacecraft subsequent to launch have been computed, and this allows the *required* launch mass of the spacecraft, m_{req} , to be calculated. This required launch mass includes the dry mass of the spacecraft, the fuel it must carry to perform the asteroid arrival and departure maneuvers, and the fuel required for the final maneuver upon Earth return if necessary, and is given by

$$m_{\text{req}} = m_{\text{dry}} e^{\left(\frac{\Delta V_{\text{ARR}_A} + \Delta V_{\text{DEP}_A} + \Delta V_{\text{RET}}}{g_{sp}^I} \right)} \quad (9)$$

Next, the program computes the *available* launch mass from the launch vehicle, m_{C_3} , as a function of the aforementioned Earth departure C_3 value using a polynomial equation that yields available launch vehicle launch mass as a function of C_3 , which is

$$m_{C_3} = p_4 (C_3)^4 + p_3 (C_3)^3 + p_2 (C_3)^2 + p_1 (C_3) + p_0 \quad (10)$$

where the polynomial coefficients p_0 through p_4 are specified in the main input file. This allows the mass ratio value for the round-trip trajectory sequence to be calculated.

The mass ratio, α_m is defined as the ratio of the required launch mass to the available launch mass and is therefore calculated by dividing the available launch mass into the required launch mass as follows

$$\alpha_m = \frac{m_{\text{req}}}{m_{C_3}} \quad (11)$$

If $\alpha_m \leq 1$ then the launch vehicle is capable of launching enough mass to inject the crew vehicle (fully loaded with all of its propellant) into the outbound trajectory for the asteroid. In this case, the round-trip trajectory solution is deemed feasible. On the other hand, if $\alpha_m > 1$, then the launch vehicle is not capable of launching the required total spacecraft mass onto the outbound trajectory and the trajectory solution is therefore deemed infeasible. This is the basis for our definition of “accessible:” *in order for an asteroid to be considered accessible, it must offer at least one trajectory solution for which $\alpha_m \leq 1$ within the range of Earth departure dates and total round-trip flight times considered.* As described previously, this accessibility definition thus depends not only on the departure dates considered and maximum round-trip flight time allowed, but also on all of the relevant vehicle performance parameters: launch vehicle capability (expressed by the launch mass vs. C_3 curve), crew vehicle dry mass, crew vehicle thruster specific impulse, and maximum crew vehicle atmospheric re-entry velocity.

If no $\alpha_m \leq 1$ round-trip trajectory solution is found for the asteroid, the program will keep track of and output the minimum mass ratio round-trip trajectory solution found for the asteroid; this represents the closest that the asteroid came to being accessible. If an asteroid never offers an outbound trajectory with a C_3 that is within specified limits, no data is output for the asteroid.

The processing steps described above are repeated for all asteroids in the population.

II.D. Distributed Parallel Processing

Performing all of these trajectory and propellant calculations for all the possible trajectory solutions for all asteroids in the population is clearly a very computationally expensive task that would ordinarily require far too much CPU time to ever be practical. However, note that all of the individual trajectory and propellant calculations for a given asteroid are completely independent of one another. Moreover, all of the calculations for a given asteroid are completely independent of the calculations for any of the other asteroids. Thus the processing algorithm is trivially parallelizable, meaning that all of its calculations can be easily deployed on separate CPUs and CPU cores. We therefore chose to take a distributed parallel processing approach in which the calculations are automatically spread over a computing cluster or network of computing nodes. This allows the massive number of required calculations to be performed relatively quickly.

The processing was coordinated, executed, and monitored on a geographically distributed computing network using the Ground Enterprise Management System (GEMS). GEMS is a product for managing, monitoring, and controlling highly distributed and reliable spacecraft ground systems. This study used the GEMS scheduler, its plug-in object architecture to define algorithm and task objects, and the system agent to coordinate activities in the distributed platform. The developed plug-in algorithm handled the distribution of tasks among the processing nodes. The task object was responsible for dispatching the computational job that executed an independently developed application (the asteroid accessibility analysis program) and captured its results on a central server.

II.E. Post-Processing

After computing all the raw accessibility data for the NEA population, a variety of post-processing steps were taken to organize and present the results. Standard plots of the trajectories were created, along with tables presenting all the key trajectory information; examples of these are presented herein with the study results. Additionally, specialized data plots were developed that attempt to visually communicate the features of the multi-dimensional round-trip trajectory trade space; examples of these and discussions of their uses and attributes are also provided with the results. The estimated sizes of the NEAs were also computed, along with the launch and return asymptotic declination angles for the outbound and inbound trajectories.

II.E.1. Estimated NEA Size

The original list of NEAs from the NASA/JPL NEO Program website includes the orbital elements and absolute magnitudes of each NEA, and we use the absolute magnitude values in post-processing to compute the estimated size range for each NEA. The NASA/JPL NEO Program website provides a table for converting absolute magnitudes to estimated size ranges, assuming an albedo of 0.25 to 0.05[†]. We perform linear interpolation on these tabulated values to compute the estimated NEA sizes.

The impact of estimated NEA size on the attractiveness of candidate NEAs for human missions is currently ill-defined. Our general thought in the beginning was that the NEA should ideally be at least approximately 200 m in mean diameter, but nature may not furnish a human-accessible NEA of that size or larger at a desired time. This issue will be studied in future work as the relevance of NEA size to human missions is considered more carefully. For now it is important to simply be cognizant of each NEA's estimated physical size, with the understanding that a given NEA may have an albedo that is quite different from the albedo range assumed in the estimated size calculations; this underscores the importance of robotic precursor missions to any NEAs that are candidates for human missions, since we cannot determine an NEA's albedo from ground observations. Robotic precursor missions would of course provide this information and much, much more.

II.E.2. Launch and Re-Entry Asymptotic Declination Angles

The asymptotic declination angles of the launch and re-entry trajectories are currently computed as a post-processing step. However, we would like to incorporate these quantities into the accessibility algorithm in future work. The launch asymptotic declination angle can affect the launch vehicle performance and range safety, and the re-entry asymptotic declination angle can affect the safety of the crew.⁵ More study is needed on these topics to determine how to incorporate the asymptotic declination angles into the accessibility algorithm mathematically. However, we present the asymptotic declination angle calculations here for completeness.

The calculations are the same for launch and re-entry; what differs is the velocity vector that is utilized in the computation. For launch, the necessary velocity vector is the hyperbolic excess velocity with respect to Earth on the outbound trajectory, \vec{v}_∞ , described in Eq. (2). For re-entry, it is the heliocentric velocity of the spacecraft relative to Earth at the time of Earth return, \vec{v}_{HE} , described in Eq. (6). The symbol \vec{v} will be used to represent either of these velocities in the asymptotic declination angle equations that follow.

First, the relevant epoch (time of Earth departure or time of Earth return) is converted from a Julian Date to Julian Centuries as follows¹³

$$T_{JC} = \frac{JD - 2451545.0}{36525} \quad (12)$$

[†]<http://neo.jpl.nasa.gov/glossary/h.html>

where JD is the time of Earth departure or Earth return in Julian Date format. The epoch in Julian Centuries is then used to compute the mean obliquity of the ecliptic, ϵ (the angle between Earth's equatorial plane and the ecliptic plane) in radians according to¹³

$$\epsilon = 0.409092802283074 - 0.000226966106587847(T_{JC}) - 2.8623399732707 \times 10^{-9}(T_{JC}^2) + 8.79645943005142 \times 10^{-9}(T_{JC}^3) \quad (13)$$

The mean obliquity is then used to form the matrix that transforms vectors from the Heliocentric Inertial (HCI) frame to the Earth-Centered Inertial (ECI) frame, given by

$$T_{ECI}^{HCI} = \begin{bmatrix} 1 & 0 & 0 \\ 0 & \cos(\epsilon) & -\sin(\epsilon) \\ 0 & \sin(\epsilon) & \cos(\epsilon) \end{bmatrix} \quad (14)$$

Next, the relevant heliocentric velocity vector (relative to Earth), \vec{v} , is transformed from the HCI frame to the ECI frame using the transformation matrix given in Eq. (14) as follows

$$\vec{v}_{ECI} = T_{ECI}^{HCI} \vec{v} \quad (15)$$

The magnitude of this vector is $v = \|\vec{v}_{ECI}\|$ and we denote the z component of the vector as v_z . Then, the asymptotic declination angle, δ , is computed according to

$$\delta = \arcsin\left(\frac{v_z}{v}\right) \quad (16)$$

III. Results

The first round of NEA processing utilized the prototype accessibility analysis software in early December of 2009 and consisted of processing the 6496 NEAs known as of November 16th, 2009, yielding 42 accessible NEAs. The total processing time was 1.5 days on geographically distributed computing nodes with a total of 39 CPU cores^u. The NEA accessibility analysis software was finalized shortly thereafter and in mid-December the 6611 NEAs known as of December 10th, 2009, were processed, yielding an additional 15 accessible NEAs and bringing the total number of accessible NEAs to 57. On February 19th, 2010, the 142 NEAs discovered since December 10th, 2009, were processed, yielding 2 more accessible NEAs and bringing the total number of accessible NEAs to 59. Processing those 142 NEAs required only 2 hours using 16 CPU cores. By March 26th, 2010, the accessibility space plotting software was complete and the project was placed on indefinite hold pending additional funding. Note that 81 NEAs were discovered between February 19th, 2010 and March 26th, 2010, but there was not sufficient personnel availability to execute processing of them. To date, 238 NEAs have been discovered since March 26th, 2010, bringing the total number of unprocessed NEAs to 319. The time history of NEA population discovery and accessibility assessments is presented in table 2. Note that the average NEA discovery rates over these time intervals demonstrate that even if NEA discovery rates increase substantially, a single standard multi-core workstation computer could perform automated accessibility assessment of new NEAs as they are discovered (e.g., on a weekly basis) and easily keep pace with NEA discovery very inexpensively.

Table 3 presents the currently known 59 accessible NEAs in decreasing order of estimated physical size. The orbital parameters (semi-major axis, eccentricity, and inclination) of these NEAs are also presented, along with the total number of distinct round-trip trajectory opportunities they offer between the years 2016 and 2050 (limited by the utilized trajectory grid size parameters). Summing the number of opportunities offered by each of the 59 accessible NEAs yields a grand total of 2,989,022 distinct round-trip mission opportunities to NEAs between 2016 and 2050. While the difference between adjacent or nearly adjacent opportunities may be trivial in some cases, the total number of opportunities serves as an indicator of the accessibility space density. Also tabulated are the minimum and maximum total round trip flight times offered by each NEA and the minimum and maximum available launch years. However, note that these

^uMany of these were older model computers due to budget limitations. If all of them had been modern CPUs with good clock speeds, the processing would have been much faster. There were a few fast modern processors in the collection of CPUs and those ended up doing the majority of the data processing since they outran the slower CPUs and hence were naturally fed more processing batch jobs by the scheduling algorithm.

Table 2. Time history of NEA population discovery and accessibility assessments.

Date	Total NEAs	New NEAs	Total Accessible NEAs	New Accessible NEAs	Average NEA Discovery Rate
11/16/2009	6496	-	42	-	-
12/10/2009	6611	115	57	15	4.8/day
02/19/2010	6753	142	59	2	2.0/day
03/26/2010	6834	81*	59+?	?	2.3/day
07/14/2010	7069	238*	59+?	?	2.2/day

* These NEAs have not yet been analyzed for accessibility.

quantities are not correlated to each other in table 3; they are simply used to quickly identify attractive accessible NEAs. For instance, if only NEAs offering a certain total round-trip flight time are desired, then it is easy to use table 3 to immediately select only those NEAs that offer at least one opportunity with a satisfactory total round-trip flight time. Likewise, if only a certain launch year or range of launch years is desired, table 3 can be used to immediately identify only those NEAs that offer round-trip trajectory opportunities with launch years that fall within the desired range. However, detailed analysis of the trajectory data files for the NEAs that pass these initial tests must then be performed to confirm that a given NEA meets the desired requirements.

Examination of table 3 was followed by examination of the relevant NEA trajectory data files to produce a list of the most attractive accessible NEAs. The goal was to identify accessible NEAs that most closely meet the following requirements: launch year between 2020 and 2030 (ideally 2025), round-trip flight time as short as possible, but at most approximately 6 months, and estimated physical size of 200 m or larger. None of the currently known accessible NEAs strictly meet all of these requirements, but the 14 of them that do meet requirements or come close in one or more ways are listed in table 4.

Note that the asteroids 2008 HU₄, 1991 VG, and 2008 EA₉ offer their short round-trip flight time trajectory opportunities with launch years < 2020, but we present these NEAs here because they are interesting. 2008 HU₄ appears to be a rather small NEA and its best opportunity has a launch year of 2016, which is far too early for a human mission. However, it offers a very short round-trip flight time of 54 days. Additionally, 2008 EA₉ offers a 36 day round-trip trajectory in the year 2049. While these examples do not achieve the desired 2025 launch year time frame, they prove that such ultra-short round-trip trajectories are truly possible and raise hopes that such opportunities will be found with launch years near 2025 as new NEAs are discovered, presuming that this NEA accessibility study is resumed and carried through to its logical conclusion. The largest of the currently known attractive accessible NEAs is 2001 QJ₁₄₂, with an estimated size of 52 - 125 m, and it offers a 180 day round-trip trajectory with a launch year of 2024.

The best-case mission opportunity (minimum mass ratio) was recorded for each of the inaccessible asteroids in the population and these were tabulated in increasing order of mass ratio. *Marginally inaccessible* NEAs were then defined as those with $\alpha_m < 1.1$, meaning that reaching these asteroids would require less than a 10% increase in launch vehicle launch mass capability, or a less than 10 % decrease in required spacecraft launch mass, or a complimentary combination thereof. A total of 10 marginally inaccessible NEAs were found and they are listed in table 5 in order of increasing mass ratio, α_m . Note that there are several marginally inaccessible NEAs, 2003 LN₆, 2007 SQ₆, 2008 LD, and 2006 WB, which offer nearly achievable mission opportunities with launch years between 2023 and 2025

III.A. Detailed Trajectory Data

One of the incredible advantages of the NEA accessibility search algorithm presented herein is that *every possible round-trip trajectory (limited by trajectory grid size parameters) to every NEA is computed in order to evaluate accessibility*. This is an especially powerful feature of the method because it automatically furnishes complete trajectory designs for all of the NEAs, requiring no additional manual trajectory design. Of course, the set of trajectory data for all of the accessible NEAs is far too dense and extensive to present here (with a total of 2,989,022 distinct trajectory solutions), so we show several of the more interesting round-trip trajectory examples.

Table 6 presents examples of complete trajectory solutions for the asteroids 2008 HU₄, 2008 EA₉, and 2001 QJ₁₄₂. Asteroid 2008 HU₄ offers an example of a very short round-trip flight time mission at 54 days,

Table 3. Listing of the 59 accessible NEAs.

Name	Est. Size (m)	a (AU)	e	i	# Opp.*	T_{tot}	Range [†] (days)	Launch Year Range [‡]	α_m	Range [§]
2008 EV ₅	274 - 600	0.959	0.084	7.436°	30		356 - 360	2024 - 2024	0.923 - 1.000	
2003 SM ₈₄	75 - 171	1.125	0.082	2.795°	939		138 - 234	2040 - 2046	0.907 - 1.000	
2001 QJ ₁₄₂	52 - 125	1.062	0.086	3.106°	617		180 - 360	2024 - 2035	0.740 - 1.000	
2009 UY ₁₉	51 - 122	1.020	0.031	9.052°	762		168 - 360	2038 - 2039	0.664 - 1.000	
2007 PS ₉	50 - 119	1.074	0.076	8.703°	484		166 - 198	2046 - 2046	0.866 - 1.000	
2009 TP	49 - 118	1.029	0.224	0.790°	14		348 - 356	2035 - 2035	0.985 - 0.999	
2009 OS ₅	49 - 116	1.144	0.097	1.695°	131		162 - 228	2020 - 2020	0.957 - 1.000	
1999 AO ₁₀	43 - 102	0.912	0.111	2.622°	127		150 - 210	2025 - 2025	0.913 - 1.000	
2006 BJ ₅₅	38 - 87	1.029	0.129	5.919°	21		356 - 360	2030 - 2030	0.902 - 0.998	
2009 CV	38 - 85	1.112	0.150	0.957°	691		210 - 270	2029 - 2029	0.878 - 1.000	
1997 YM ₉	37 - 82	1.095	0.104	7.842°	182		168 - 198	2044 - 2044	0.913 - 1.000	
2005 UG ₅	36 - 80	1.056	0.190	2.866°	175		348 - 360	2043 - 2043	0.828 - 1.000	
2001 FR ₈₅	35 - 75	0.983	0.028	5.245°	52,143		142 - 360	2038 - 2040	0.499 - 1.000	
2007 CS ₅	35 - 75	0.980	0.173	0.745°	4,719		288 - 360	2040 - 2043	0.679 - 1.000	
2009 YF	31 - 69	0.935	0.121	1.525°	2,396		204 - 310	2019 - 2047	0.779 - 1.000	
2007 WA	31 - 69	1.035	0.153	6.164°	20		354 - 360	2028 - 2028	0.958 - 0.995	
2009 HC	30 - 67	1.039	0.126	3.778°	14,303		280 - 360	2025 - 2043	0.640 - 1.000	
2007 YF	30 - 67	0.953	0.120	1.653°	5,485		226 - 360	2021 - 2047	0.764 - 1.000	
2005 TG ₅₀	29 - 67	0.924	0.134	2.427°	1,192		214 - 360	2021 - 2044	0.899 - 1.000	
2000 SG ₃₄₄	29 - 66	0.977	0.066	0.110°	708,703		96 - 360	2027 - 2030	0.363 - 1.000	
2002 PN	29 - 66	1.015	0.069	9.144°	310		342 - 360	2048 - 2049	0.638 - 1.000	
2009 BW ₂	24 - 57	1.019	0.139	1.011°	5,724		240 - 360	2042 - 2043	0.720 - 1.000	
1999 CG ₉	23 - 57	1.061	0.062	5.158°	1,607		162 - 360	2033 - 2045	0.716 - 1.000	
2000 AG ₆	22 - 53	1.018	0.190	2.435°	436		340 - 360	2041 - 2041	0.867 - 1.000	
2006 BZ ₁₄₇	21 - 51	1.024	0.099	1.409°	45,178		192 - 360	2034 - 2037	0.450 - 1.000	
2008 JE	18 - 41	0.984	0.093	6.965°	278		336 - 360	2045 - 2046	0.814 - 0.999	
2006 QQ ₅₆	18 - 40	0.985	0.045	2.797°	241,961		96 - 360	2049 - 2051	0.432 - 1.000	
2006 UB ₁₇	15 - 33	1.141	0.104	1.991°	636		132 - 228	2045 - 2045	0.896 - 1.000	
2009 DB ₄₃	13 - 31	1.102	0.172	0.934°	2,921		262 - 360	2045 - 2045	0.741 - 1.000	
2006 HE ₂	13 - 30	1.065	0.157	1.180°	4,500		288 - 360	2017 - 2028	0.777 - 1.000	
2007 VU ₆	13 - 29	0.976	0.091	1.223°	37,325		238 - 360	2033 - 2036	0.596 - 1.000	
2005 UV ₆₄	12 - 28	0.958	0.116	5.416°	448		322 - 360	2035 - 2035	0.788 - 1.000	
1999 VX ₂₅	12 - 28	0.900	0.140	1.663°	2,408		150 - 276	2028 - 2046	0.747 - 1.000	
2008 EY ₈₄	12 - 27	1.030	0.175	4.333°	21		356 - 360	2030 - 2030	0.931 - 0.998	
2005 LC	12 - 26	1.133	0.102	2.800°	649		144 - 228	2039 - 2040	0.861 - 1.000	
2008 DL ₄	12 - 26	0.929	0.123	3.206°	137		324 - 360	2016 - 2016	0.933 - 1.000	
2001 GP ₂	11 - 25	1.038	0.074	1.279°	109,246		162 - 360	2019 - 2049	0.474 - 1.000	
2006 DQ ₁₄	11 - 24	1.028	0.053	6.297°	8,665		154 - 360	2029 - 2030	0.660 - 1.000	
2008 ST	11 - 23	0.964	0.126	1.906°	32,177		234 - 360	2025 - 2042	0.761 - 1.000	
2007 XB ₂₃	11 - 23	1.041	0.054	8.530°	9,816		148 - 360	2024 - 2025	0.535 - 1.000	
2000 SZ ₁₆₂	10 - 23	0.930	0.168	0.893°	1,249		240 - 360	2017 - 2042	0.860 - 1.000	
2009 UD	10 - 23	1.039	0.122	4.410°	3,072		300 - 360	2028 - 2045	0.624 - 1.000	
2006 UQ ₂₁₆	9 - 21	1.104	0.162	0.473°	5,363		192 - 360	2021 - 2050	0.741 - 1.000	
2008 EA ₉	8 - 17	1.059	0.080	0.424°	410,081		36 - 360	2019 - 2049	0.459 - 1.000	
2007 BB	7 - 16	0.933	0.141	3.529°	30		336 - 360	2033 - 2033	0.967 - 0.999	
2004 QA ₂₂	7 - 16	0.951	0.122	0.576°	21,024		196 - 360	2017 - 2043	0.631 - 1.000	
2009 YR	7 - 15	0.942	0.112	0.711°	41,397		174 - 360	2019 - 2042	0.615 - 1.000	
2008 EL ₆₈	7 - 15	1.210	0.192	0.577°	61		180 - 234	2036 - 2037	0.944 - 0.999	
2003 WT ₁₅₃	7 - 15	0.894	0.178	0.371°	309		208 - 252	2030 - 2030	0.872 - 1.000	
2008 CM ₇₄	7 - 15	1.089	0.147	0.855°	5,736		216 - 360	2016 - 2050	0.718 - 1.000	
2008 HU ₄	6 - 14	1.097	0.078	1.322°	94,479		54 - 360	2016 - 2047	0.574 - 1.000	
2009 WR ₅₂	6 - 13	1.033	0.155	4.239°	797		334 - 360	2028 - 2032	0.717 - 1.000	
2008 GM ₂	6 - 13	1.052	0.157	4.096°	612		290 - 360	2034 - 2044	0.878 - 1.000	
1991 VG	5 - 13	1.026	0.049	1.445°	274,560		138 - 360	2016 - 2039	0.439 - 1.000	
2007 UN ₁₂	5 - 11	1.053	0.060	0.234°	221,170		156 - 360	2020 - 2049	0.475 - 1.000	
2000 LG ₆	4 - 9	0.917	0.111	2.833°	2,220		138 - 360	2028 - 2036	0.803 - 1.000	
2008 UA ₂₀₂	3 - 7	1.033	0.068	0.264°	132,719		210 - 360	2028 - 2045	0.444 - 1.000	
2006 RH ₁₂₀	3 - 7	1.033	0.024	0.595°	373,546		66 - 360	2027 - 2044	0.467 - 1.000	
2008 JL ₂₄	3 - 7	1.038	0.107	0.550°	103,020		150 - 360	2024 - 2044	0.465 - 1.000	

* The number of opportunities is specific to the embedded trajectory grid step sizes.

† The minimum and maximum round-trip flight times are not correlated to the min and max launch years or the min and max mass ratios; rather, they are simply the min and max round-trip flight times available overall for the NEA.

‡ The minimum and maximum round-trip launch years are not correlated to the min and max round-trip flight times or the min and max mass ratios; rather, they are simply the min and max launch years available overall for the NEA.

§ The minimum and maximum mass ratios are not correlated to the min and max round-trip flight times or the min and max launch years; rather, they are simply the min and max mass ratios available overall for the NEA.

Table 4. Listing of the 14 most attractive accessible NEAs and their best mission opportunities.

Name	Est. Size (m)	Launch Year	T_{tot} (days)
2008 HU ₄	6 - 14	2016	54
1991 VG	5 - 13	2017	138
2008 EA ₉	8 - 17	2019	132
2008 EA ₉		2049	36
2009 OS ₅	49 - 116	2020	162
2007 UN ₁₂	5 - 11	2020	178
2001 GP ₂	11 - 25	2020	186
2007 XB ₂₃	11 - 23	2024	148
2001 QJ ₁₄₂	52 - 125	2024	180
1999 AO ₁₀	43 - 102	2025	150
2008 JL ₂₄	3 - 7	2026	150
2006 RH ₁₂₀	3 - 7	2028	66
2006 UQ ₂₁₆	9 - 21	2028	192
2000 SG ₃₄₄	29 - 66	2029	96
2006 DQ ₁₄	11 - 24	2030	154

Table 5. Listing of the 10 marginally inaccessible NEAs and their best-case mission opportunities.

Name	Est. Size (m)	Launch Date	T_{tot} (days)	C_3 (km ² /s ²)	Total Post-EDS ΔV (m/s)	v_{ret} (km/s)	α_m
2003 LN ₆	35 - 77	11/27/2025	204	1.54	3475	11.778	1.00325
2001 CQ ₃₆	77 - 174	01/18/2031	296	15.34	2801	11.974	1.01340
2004 JN ₁	52 - 123	11/12/2037	314	10.30	3081	11.788	1.01966
2007 UY ₁	70 - 160	09/03/2032	350	19.30	2633	12.000	1.02698
2004 FM ₃₂	13 - 29	09/28/2033	360	16.58	2787	11.531	1.03017
2007 SQ ₆	114 - 252	10/09/2023	360	28.62	2182	12.000	1.04471
2008 LD	4 - 10	05/24/2024	192	16.30	2871	11.653	1.05361
2006 WB	72 - 164	05/30/2024	180	5.25	3465	11.881	1.06232
2005 QP ₁₁	14 - 31	03/11/2029	360	12.78	3145	12.000	1.08493
2003 RU ₁₁	19 - 47	03/03/2034	200	13.90	3103	11.918	1.09098

launching in the year 2016, and asteroid 2008 EA₉ offers an even shorter round-trip flight time of 36 days, launching in the year 2049. Of course, those launch years are too early and too late, respectively, to be truly attractive, but they provide concrete evidence that nature admits of such short round-trip missions, fueling our hopes of discovering such an opportunity with a launch year in the mid-2020s to a somewhat larger asteroid as NEAs continue to be discovered. Asteroid 2001 QJ₁₄₂ is perhaps the most attractive NEA we have found, offering a 6 month round-trip flight time to an asteroid that is up to 125 m in size, and with a launch year of 2024.

Table 6. Example trajectory solutions for the asteroids 2008 HU₄, 2008 EA₉, and 2001 QJ₁₄₂.

	Units	2008 HU ₄	2008 EA ₉	2001 QJ ₁₄₂
Est. Size	m	6 - 14	8 - 17	52 - 125
T_{tot}	days	54	36	180
Launch Date		04/12/2016	01/01/2049	04/24/2024
Departure C_3	km ² /s ²	2.086	0.555	5.391
δ_{DEP}^*		-10.461°	-15.223°	38.469°
TOF _{EA}	days	22	22	88
ΔV_{ARR_A}	m/s	1066	1975	1184
A _{STAY}	days	4	4	4
ΔV_{DEP_A}	m/s	2230	1405	2074
TOF _{AE}	days	28	10	88
δ_{RET}		4.841°	15.270°	-50.517°
v_{ret}	km/s	11.147	11.158	11.356
α_m		0.95491	0.95693	0.99566

* The DEP and RET subscripts on the asymptotic declination angles in this table refer to Earth departure and Earth return, respectively.

Figures 4, 5, and 6 present the round-trip heliocentric frame trajectory plots (ecliptic plane projections) corresponding to the trajectory solutions given in table 6 for asteroids 2008 HU₄, 2008 EA₉, and 2001 QJ₁₄₂, respectively. Broadened red arcs in figures 4, 5, and 6 denote spacecraft loiter intervals at the corresponding NEAs.

III.B. Accessibility Space Plots

Visually communicating the nature of a given NEA’s accessibility space using some sort of data plot turned out to be particularly challenging. Ordinarily, all of the possible one-way trajectories to a NEA can be easily visualized with a so-called “Pork Chop Contour” (PCC) plot. The PCC is a common trajectory design tool and allows easy communication of the entire one-way accessibility space for a NEA. Moreover, it facilitates easy trajectory optimization (the best-performing trajectory or set of trajectories can be easily seen on the plot). Thus the PCC will be a primary data product for forthcoming NEA robotic precursor mission studies.

However, we found that the PCC was an ineffective visual communication tool for round-trip trajectory accessibility spaces. The problem is that the PCC typically consists of contours on the surface defined by departure date and one-way flight time since it maps directly to a standard single trajectory grid (e.g., the outer grid in figure 2). As described previously, we necessarily utilize the method of embedded trajectory grids to compute all possible round-trip trajectory solutions, adding the extra dimensions associated with the array of embedded grids for asteroid stay time and flight time to return to Earth. Thus there are too many dimensions to be represented on a two-dimensional contour plot. To further complicate the issue, there can be (and generally are) multiple round-trip trajectory solutions with different mass ratios but identical Earth departure dates and total round-trip flight times.

Our solution was to create four types of complimentary accessibility space plots, yielding four plots per accessible NEA. These plots were generated for all of the accessible NEAs, and an example of each plot type for the asteroid 2007 XB₂₃ is presented and discussed in turn.

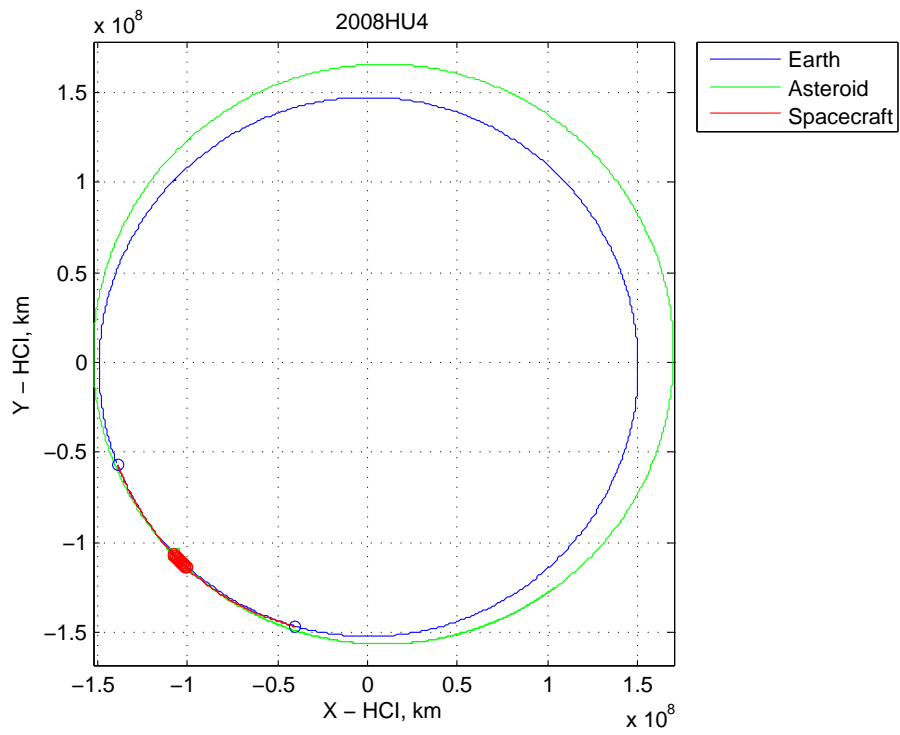


Figure 4. 54 day round-trip trajectory to asteroid 2008 HU₄ launching in the year 2016.

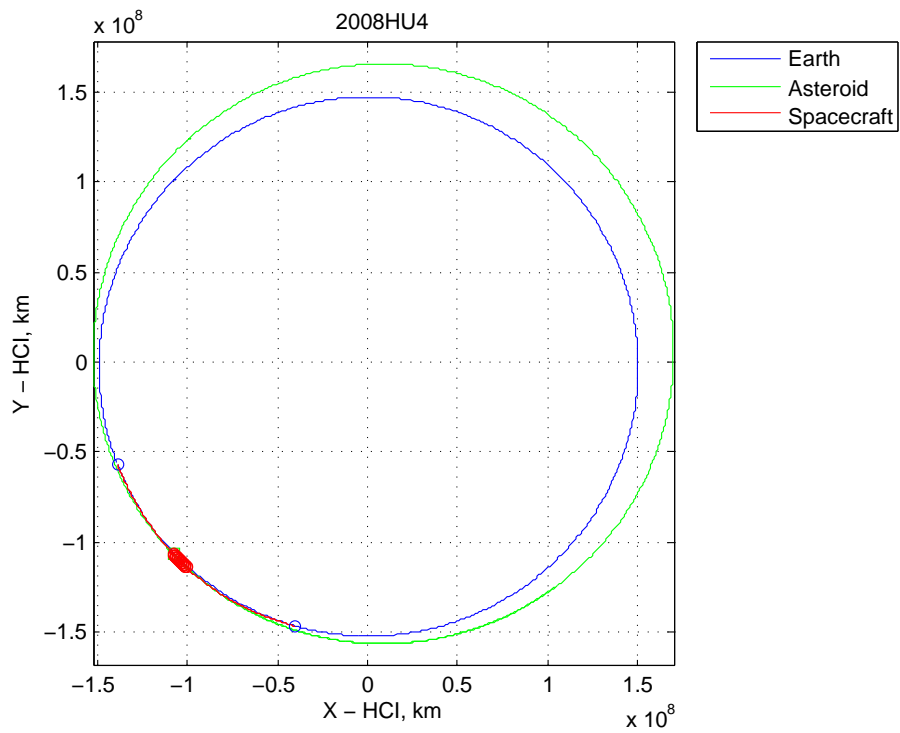


Figure 5. 36 day round-trip trajectory to asteroid 2008 EA₉ launching in the year 2049.

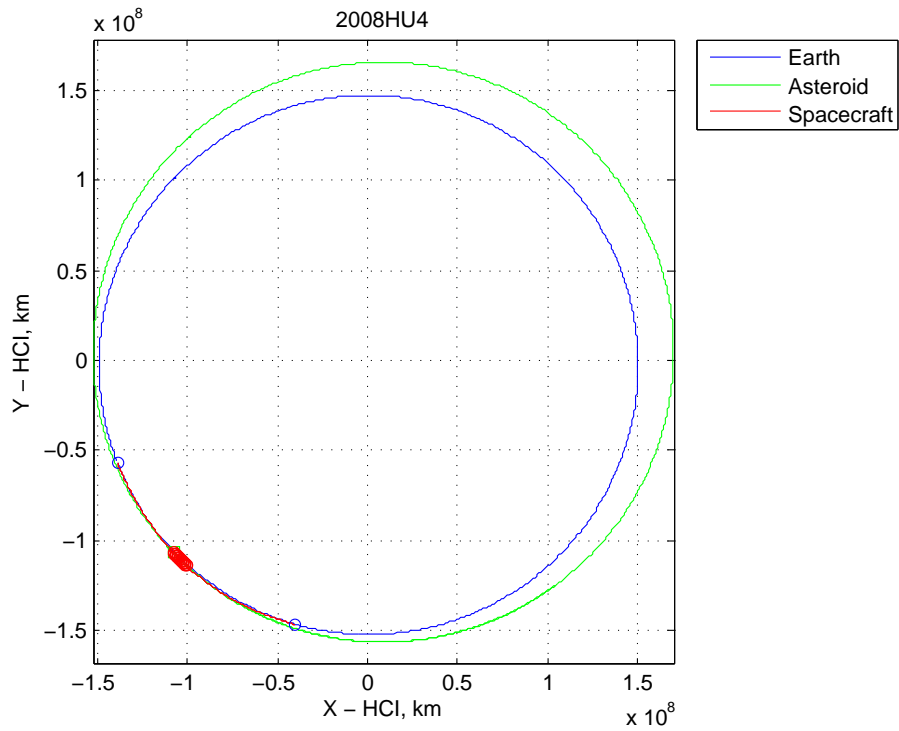


Figure 6. 180 day round-trip trajectory to asteroid 2001 QJ₁₄₂ launching in the year 2024.

III.B.1. 3D Mass Ratio Plot

The 3D mass ratio plot, presented in figure 7, shows the overall accessibility space, except for stay time at the asteroid. However, the 3D perspective makes it difficult to see exact ranges of available total round-trip flight times. Likewise, exact mission opportunity windows as a function of Earth departure date are difficult to see. What is apparent in this plot is the fact that multiple opportunities exist that meet the mass ratio constraint for various combinations of Earth departure date and round-trip flight time. Note that the color scale in this plot and the other accessibility space plots is indicative of the mass ratio value. A color scale bar showing the mapping of color to mass ratio value is provided on the other 2D accessibility space plots that follow.

III.B.2. Time of Flight vs. Departure Date

The time of flight vs. Earth departure date plot in figure 8 clearly shows the mission opportunity windows as a function of departure date. Additionally, this plot clearly shows the range of available total round-trip flight times as a function of departure date. However, this plot obscures the variations in mass ratio across the set of feasible trajectories. This plot may be the most useful for mission analysis purposes.

III.B.3. Mass Ratio vs. Departure Date

The mass ratio vs. departure date plot shown in figure 9 also clearly shows mission opportunity windows as a function of Earth departure date. Additionally, it shows the range of available mass ratios and correlates them to departure date. However, the variation in total round-trip flight time across the set of feasible trajectories cannot be shown.

III.B.4. Mass Ratio vs. Time of Flight

The mass ratio vs. total round-trip flight time plot in figure 10 clearly shows how the mass ratio varies as a function of total round-trip flight time across the entire trajectory data set, but the correlation to Earth

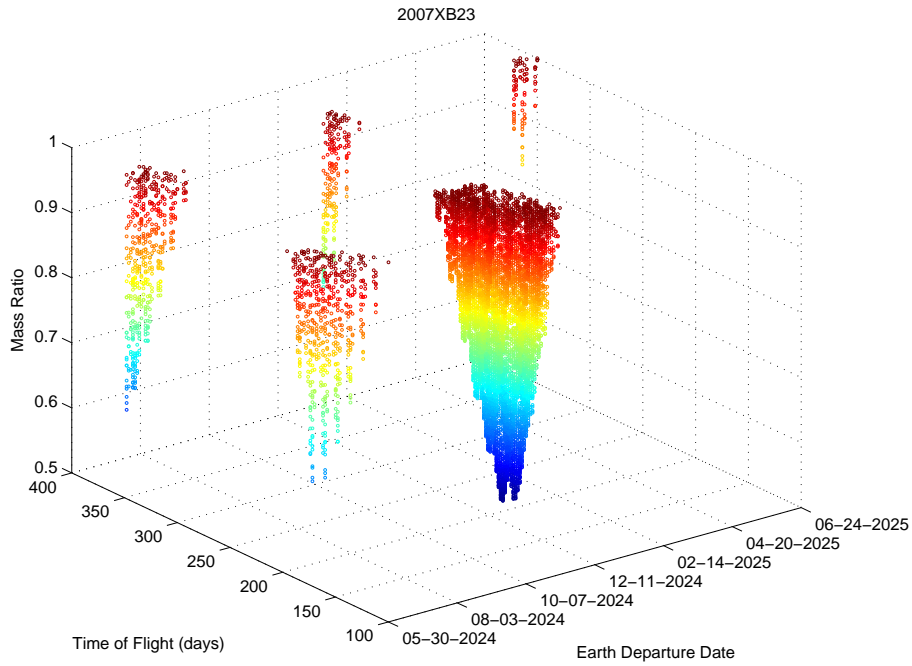


Figure 7. 3D mass ratio plot for asteroid 2007 XB₂₃.

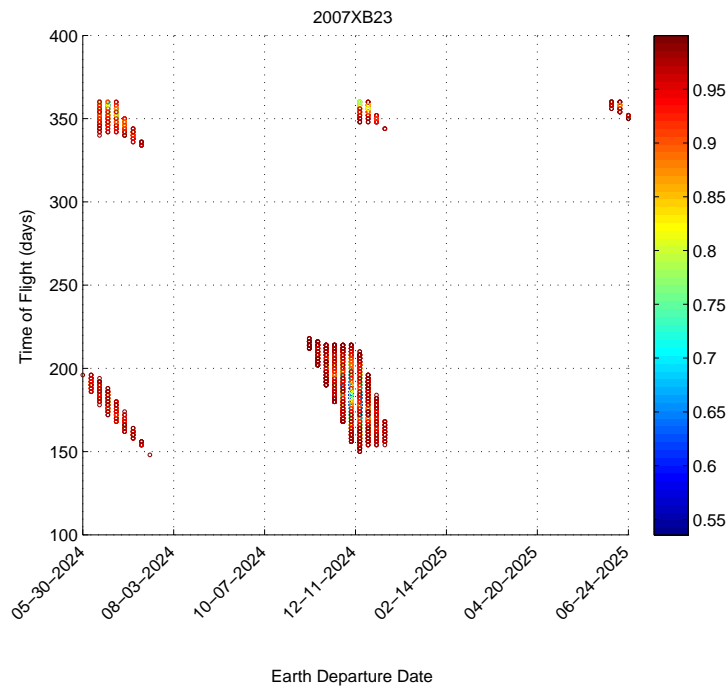


Figure 8. Total round-trip flight time vs. Earth departure date plot for asteroid 2007 XB₂₃.

departure date cannot be shown. This plot provides a good measure of how mass efficient the trajectories can be.

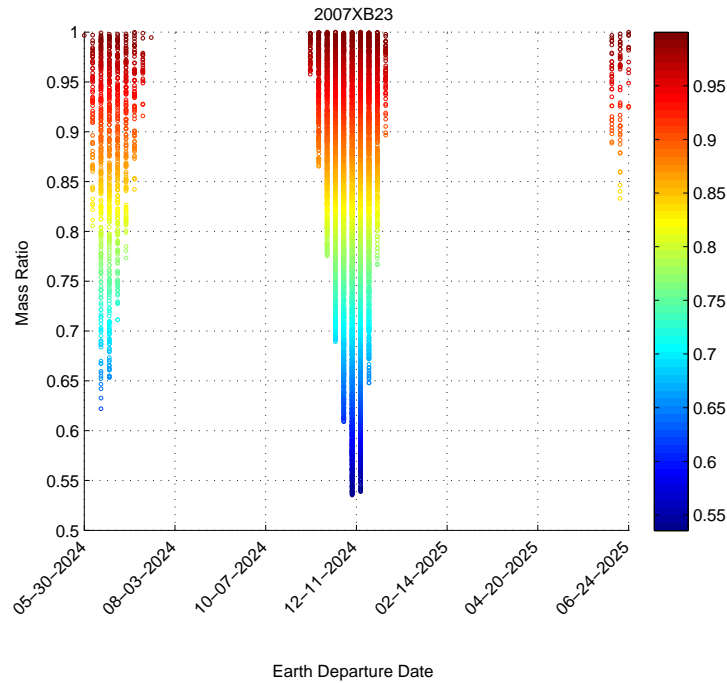


Figure 9. Mass ratio vs. Earth departure date plot for asteroid 2007 XB₂₃.

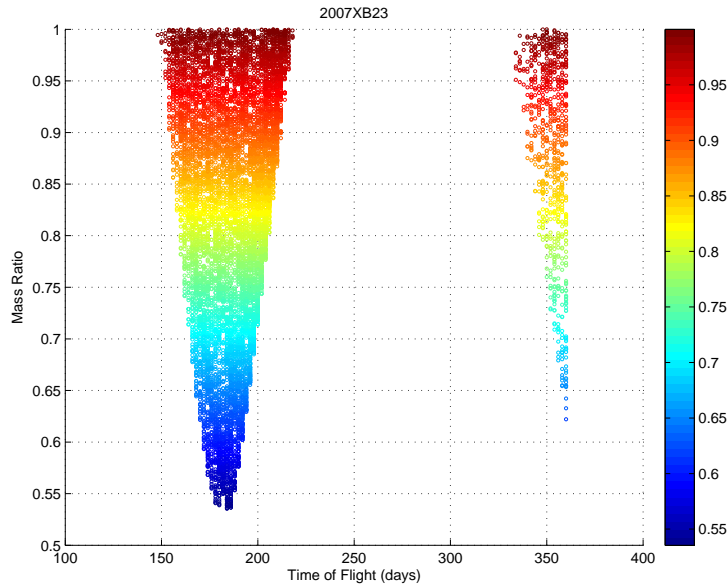


Figure 10. Mass ratio vs. total round-trip flight time plot for asteroid 2007 XB₂₃.

III.C. Rapid Sample Return Missions

While the accessibility analysis algorithm was developed to search for human mission opportunities, the algorithm and software are general enough to search for round-trip mission opportunities to NEAs for any purpose. One obvious purpose would be sample return missions. This is a particularly interesting application since we have seen that a vast multitude of mission opportunities (nearly 3 million) are available for round-trip missions to NEAs between the years 2016 and 2050, all with total round-trip flight times of 1 year or less—usually on the order of 6 to 9 months but often as low as several months or less. If these missions

were launched with small, low-cost launch vehicles, it would be conceivable to deploy a small robotic sample return spacecraft similar to the Japanese Hayabusa spacecraft that recently returned from the NEA Itokawa. Such missions would be a tremendous boon for asteroid science, offering low-cost opportunities to rapidly collect asteroid material samples.

It would be a straightforward matter to change the search parameters in the main input file and re-execute the program to search for robotic sample return opportunities. The launch vehicle launch mass polynomial coefficients could be set appropriately for a Delta II rocket, or something even smaller, such as a Minotaur V, the thruster specific impulse could be set appropriately (generally between 250 and 314 s), and the spacecraft dry mass could also be set appropriately. Departure date and other trajectory grid sizing parameters could also be modified as desired. The data processing would then yield all of the opportunities for rapid, low-cost sample return missions to the NEA population.

We have not had the time or funding to do this, but we recommend it for future work. However, we have used the existing round-trip trajectory data for several of the more interesting human-accessible NEAs to compute just how much spacecraft dry mass could be sent out on rapid sample return missions to these NEAs. The results for the asteroids 2008 HU₄, 2001 QJ₁₄₂, and 2008 EV₅ are shown in table 7.

Table 7. Example achievable spacecraft dry masses for sample return missions using a Delta II launch vehicle.

Asteroid	Launch Date	T_{tot} (days)	m_{dry} (kg) with $I_{sp} = 250$ s	m_{dry} (kg) with $I_{sp} = 314$ s
2008 HU ₄	04/12/2016	54	308	405
2001 QJ ₁₄₂	04/24/2024	180	292	383
2008 EV ₅	06/29/2024	360	297	366

Note that the average dry mass of previous asteroid science spacecraft is approximately 400 kg, and the dry mass of the recently returned Hayabusa spacecraft was 380 kg. Also, for reference, the thruster I_{sp} of the NEAR spacecraft (which traveled to the asteroid Eros) was 313 s. Thus the achievable dry mass values in table 7 are quite reasonable. Even better results would be obtained after re-processing the NEA population to specifically look for all of the robotic sample return opportunities, especially considering that the average minimum mass ratio for the currently known accessible NEAs is 0.73 and the overall minimum mass ratio is 0.36; highly efficient round-trip trajectories with total flight times of 1 year or less are clearly achievable.

These results are even more interesting when we consider that the total round-trip mission time for Hayabusa was 7 years, compared to the 54 day, 180 day, and 360 day sample return opportunities shown here; considerable mission operations cost savings would be realized with such short missions. Moreover, such missions could be deployed much more frequently since their total times are so short. It is also important to note that these results strongly imply that one-way scientific precursor mission opportunities to the human-accessible NEAs are likely to generally be extraordinarily efficient.

A sample return mission to the asteroid 2008 EV₅ might be of particular scientific interest since it is the largest of the currently known 59 human-accessible NEAs. This asteroid approached Earth to within 8.4 lunar distances during December of 2008 and was observed with delay-Doppler imaging at Goldstone and Arecibo, and with the VLBA at Green Bank. A 3D radar shape model at 7.5 m resolution for this asteroid was recently developed¹⁴ which shows the asteroid to be an oblate spheroid with an effective diameter of 450 ± 40 m, a slight equatorial ridge, a prominent concavity 100 - 200 m across, and an estimated spin period of approximately 3.7 hours. For reference, an example round-trip trajectory solution for this asteroid is presented in table 8 and the corresponding trajectory plot is shown in figure 11.

III.D. Scientific Robotic Precursor Missions

As described previously, the PCC plot is a common trajectory design tool used to quickly understand the accessibility space for one-way trajectories to NEAs and identify optimal trajectory solutions. The one-way PCC plot for a given NEA represents all of the available trajectories for robotic scientific precursor missions. For myriad reasons, not the least of which is crew safety, a robotic precursor mission would surely be sent to any candidate human-accessible NEA well in advance of the crew launch date.

We have written the computer code necessary to generate and analyze these PCC plots using the standard single trajectory grid method, though we have not yet integrated it with the accessibility analysis algorithm. In future work we hope to add the one-way PCC plot generation to the current accessibility analysis software

Table 8. Example trajectory solution for asteroid 2008 EV₅.

	Units	2008EV5
Est. Size	m	410 - 490
T_{tot}	days	360
Launch Date		06/29/2024
Departure C_3	km^2/s^2	18.746
δ_{DEP}		-17.4°
TOF_{EA}	days	148
ΔV_{ARRA}	m/s	1598
A_{STAY}	days	40
ΔV_{DEPA}	m/s	931
TOF_{AE}	days	172
δ_{RET}		-39.4°
v_{ret}	km/s	4.169
α_m		0.983

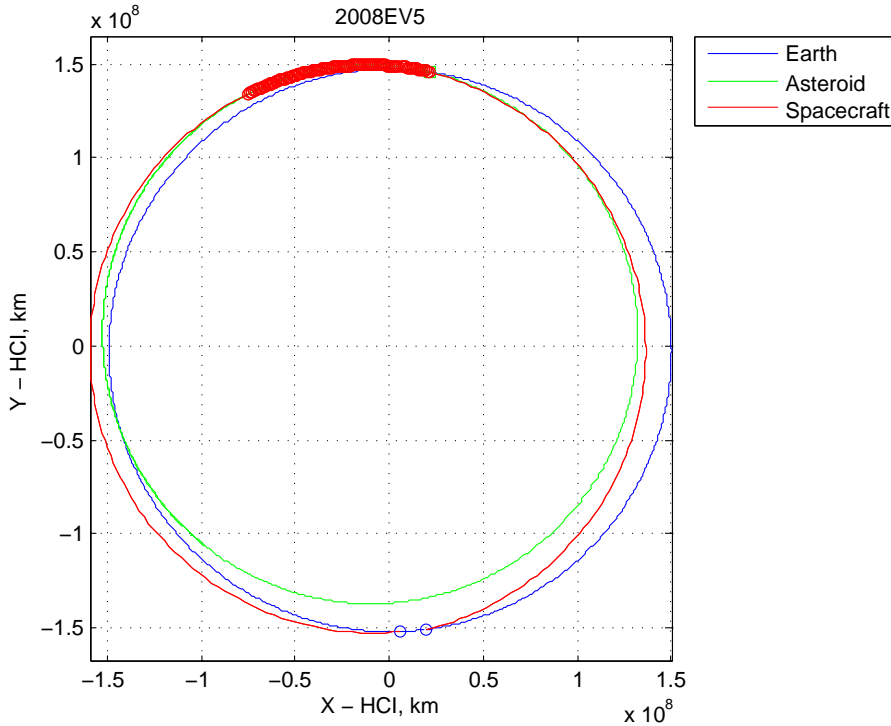


Figure 11. 360 day round-trip trajectory to asteroid 2008 EV₅ launching in the year 2024.

so that in addition to the full set of all possible round-trip trajectories, the software will also automatically generate all of the one-way robotic precursor mission trajectories to each accessible NEA.

We find it useful to generate PCC plots so that they display deliverable payload mass as a function of Earth departure date and flight time. Other parametrizations are more common, such as total ΔV , but we feel that this is less instructive as it is rarely obvious as to how total ΔV maps to the ability of a given launch vehicle and spacecraft thruster to deliver a spacecraft of a given dry mass to rendezvous with an NEA. Optimizing on delivered spacecraft dry mass allows the performance of any combination of launch

vehicle and thruster specific impulse to be immediately evaluated for the mission; clearly, the combination of launch vehicle and thruster specific impulse must allow a minimum science mission spacecraft dry mass to be delivered to rendezvous with the NEA. Here we present a previously generated example of this type of PCC plot, shown in figure 12, for the asteroid Apophis using the launch mass versus C_3 curve for the Boeing Delta II 2925-9.5 launch vehicle and a 300 second thruster specific impulse.

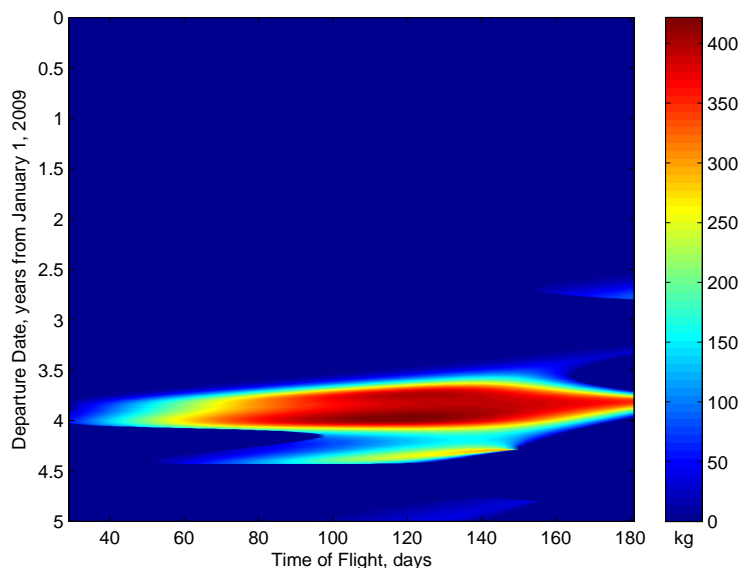


Figure 12. Example Pork Chop Contour plot for short one-way trajectories to the asteroid Apophis.

For this simple example, the year of Earth departure was constrained to be between 2009 and 2014, and the flight time was constrained to be between 30 and 180 days. The maximum delivered payload mass trajectory solution was found to be 421.63 kg with a launch date of December 23rd, 2012, an Earth departure C_3 of 16.885 km²/s², an arrival ΔV of 2118 m/s, and a flight time of 118 days. Note that a 421.63 kg NEA science spacecraft dry mass is on par with historical NEA science missions. While this simple example focuses on a relatively narrow range of Earth departure dates, when a larger range of departure dates is processed (as is usually the case) it always reveals the periodicity of the available launch windows for the NEA, which tend to repeat at approximately the synodic period between the Earth and the asteroid (for Apophis, the synodic period is approximately 8 years).

While there was not adequate time or funding for this study to produce robotic science precursor mission PCC plots for the more attractive human-accessible NEAs, we have calculated several optimal^v one-way trajectories to selected human-accessible NEAs to illustrate how efficient these missions can be (and generally are). Optimal trajectories were computed for the NEAs 1999 AO₁₀, 2001 QJ₁₄₂, 2007 XB₂₃, 2009 OS₅, and 2000 SG₃₄₄ with launch dates between 2014 and 2018, inclusive, and assuming a spacecraft thruster I_{sp} of 300 s. The results are shown in table 9.

Table 9. Example optimal robotic science precursor mission trajectory solutions for selected NEAs.

	1999 AO ₁₀		2001 QJ ₁₄₂	2007 XB ₂₃	2009 OS ₅	2000 SG ₃₄₄	
Launch Date	04/02/2016	06/09/2018	04/27/2014	01/01/2014	07/28/2014	09/19/2016	09/19/2018
Departure C_3 (km ² /s ²)	5.646	0.160	4.443	12.711	1.871	7.867	5.879
δ_{DEP}	-5.377°	18.357°	2.429°	-20.411°	-31.005°	20.891°	20.520°
TOF _{EA} (days)	432	258	404	496	326	490	466
ΔV_{ARR_A} (m/s)	4303	2595	1592	4239	940	3164	2791
Launch Mass with $m_{dry} = 220$ kg	949	464	378	929	303	645	568
Launch Mass with $m_{dry} = 400$ kg	1726	844	687	1690	551	1172	1032

The required launch masses were computed twice, once for a spacecraft dry mass of 220 kg and again for

^vIn this case optimal means minimum total ΔV (the sum of the Earth departure and NEA arrival maneuvers). In future work we will maximize spacecraft dry mass delivered to the NEA, which is slightly different in a subtle but important way.

a spacecraft dry mass of 400 kg. The former is the dry mass of the Foresight spacecraft designed by the team that won the 2007 Apophis Mission Design competition^w and the latter is the dry mass typical of historical missions to small bodies. Note that the required launch masses and C_3 values in table 9 are quite practical and serve to exemplify the efficiency with which NEAs, particularly the human-accessible NEAs, may be visited by robotic spacecraft. The maximum required launch mass for a 220 kg dry mass in table 9 is 949 kg, launching to 1999 AO₁₀ in 2016, and the minimum is 303 kg, launching to 2009 OS₅ in 2014. For the 400 kg dry mass cases, the maximum required launch mass is 1726 kg and the minimum is 551 kg. Consequently, these mission opportunities would only require relatively small and inexpensive launch vehicles, such as the Minotaur V, Falcon 9, or Delta II series. For example, the 2014 mission to 2001 QJ₁₄₂ with a 220 kg science spacecraft could theoretically be launched by a Minotaur V, while a 400 kg spacecraft for that mission could theoretically be launched by a Delta II 2920H-9.5. The trajectory plot for this mission is shown in figure 13.

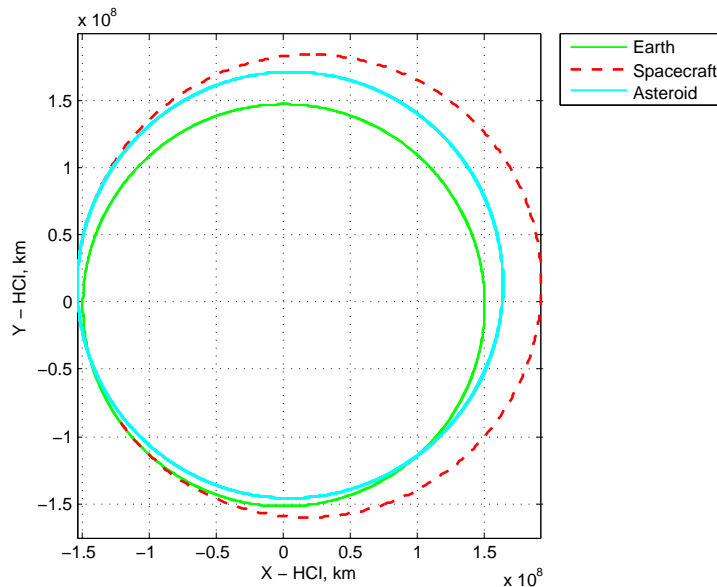


Figure 13. Robotic science precursor mission trajectory to the NEA 2001 QJ₁₄₂ launching in 2014.

III.E. Multi-Target Asteroid Missions

A robotic precursor science mission would be most useful if it was capable of visiting and surveying more than one NEA during the course of a single mission within a reasonable time frame. Visiting several or more NEAs with a single spacecraft launch would dramatically increase the ratio of science return to mission cost and thus be of tremendous aid to any precursor surveys of attractive candidate NEAs for human missions. An algorithm known as the Series Method was previously developed specifically for finding near-optimal solutions to the orbital version of the famous “Traveling Salesman” problem, thereby permitting such multi-destination missions to be designed. This algorithm was originally developed for and successfully applied to multi-asteroid rendezvous and intercept problems.¹⁵ It was later successfully applied to the problem of mission design for the re-fueling of multiple spacecraft in geostationary orbit¹⁶ (with and without the use of an orbital fuel depot), as well as the problem of orbital debris removal.¹⁷ Two preliminary example multi-NEA mission designs are included herein, and we recommend thorough analysis of multi-destination precursor science missions to the human-accessible NEAs for future work.

III.E.1. Mission Design to Visit Three Human-Accessible NEAs

This mission design was focused on visiting some of the more attractive NEAs from table 4, with an emphasis on ensuring that 2001 QJ₁₄₂ be included in the mission itinerary since it is one of the most attractive candidates for a human mission as it appears to be the largest human accessible NEA and offers a 6 month

^whttp://www.planetary.org/programs/projects/apophis_competition/

round-trip mission opportunity launching in the year 2024. An emphasis was also placed on keeping the spacecraft launch mass low in the interests of being accommodated by a relatively affordable launch vehicle.

The resulting mission design visits three NEAs in the following order: 2009 OS₅, 2001 QJ₁₄₂, and 2000 SG₃₄₄. The mission launches on July 28th, 2014, with an Earth departure C_3 of 1.871 km²/s² and a δ_{DEP} of -31.005° , arrives at 2009 OS₅ on June 19th, 2015, visits 2001 QJ₁₄₂ next, and concludes after arriving at 2000 SG₃₄₄ on July 7th, 2018, yielding a total mission duration of approximately 4.5 years, assuming that some time will be spent studying 2000 SG₃₄₄ after arrival.

Assuming a spacecraft thruster I_{sp} of 300 s, the launch mass for the mission is 2073 kg if the spacecraft dry mass is 220 kg. If the spacecraft dry mass is 400 kg, the launch mass is 3769 kg. Thus the launch mass for the 220 kg spacecraft is just slightly more than what a Falcon 9 launch vehicle can accommodate, but can be launched by either the smallest Delta IV series launch vehicle (the 4040-12) or the smallest Atlas V series launch vehicle (the 501), with several hundred kg of launch mass margin on either launch vehicle. The launch mass for the 400 kg spacecraft can be accommodated by the Delta IV 4240-12.

The mission itinerary is summarized in table 10 and a plot showing the mission trajectories (ecliptic plane projection) is presented in figure 14.

Table 10. Preliminary mission design to visit three human-accessible NEAs.

Starting Location	Destination	Departure Date	Flight Time (days)	Stay Time (days)	ΔV_{DEP} (m/s)	ΔV_{ARR} (m/s)
Earth	2009 OS ₅	07/28/2014	326	206	($C_3 = 1.871 \text{ km}^2/\text{s}^2$)	940
2009 OS ₅	2001 QJ ₁₄₂	01/11/2016	320	336	1214	839
2001 QJ ₁₄₂	2000 SG ₃₄₄	10/28/2017	252	-	2016	1592

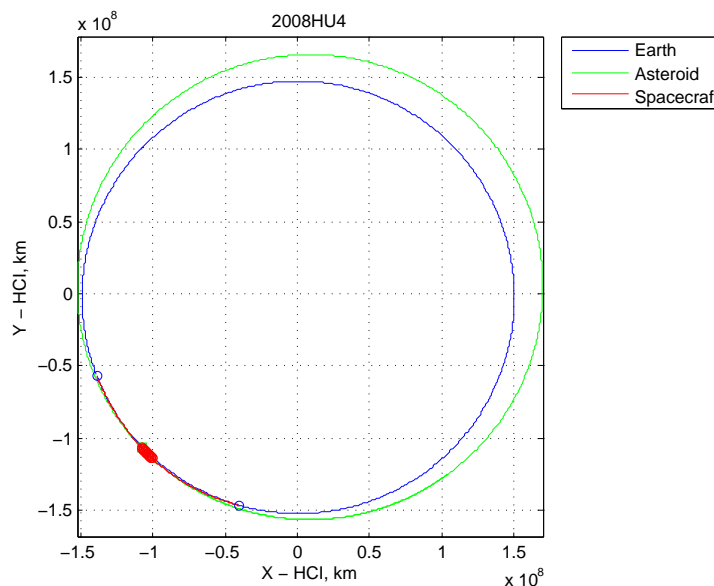


Figure 14. Trajectories for a robotic science tour of three human-accessible NEAs launching in 2014.

III.E.2. Mission Design to Visit Four Human-Accessible NEAs

As before, this mission design was focused on visiting some of the more attractive NEAs from table 4 with a relatively low launch mass, but this time there was no emphasis placed on visiting specific NEAs. The resulting mission design visits four NEAs in the following order: 1991 VG, 2008 EA₉, 2007 UN₁₂, and 2001 GP₂.

The mission launches on December 11th, 2017, with an Earth departure C_3 of 0.790 km²/s², and a δ_{DEP} of 44.934° , arrives at 1991 VG on November 4th, 2018, visits 2008 EA₉ next, and then 2007 UN₁₂. The mission concludes by arriving at 2001 GP₂ on May 5th, 2022, yielding a total mission duration of approximately 5 years, assuming that some time will be spent studying 2001 GP₂ after arrival.

Assuming a spacecraft thruster I_{sp} of 300 s, the launch mass for the mission is 1970 kg if the spacecraft dry mass is 220 kg. If the spacecraft dry mass is 400 kg, the launch mass is 3582 kg. Thus the launch mass for the 220 kg spacecraft can be accommodated by a Falcon 9 launch vehicle. The launch mass for the 400 kg spacecraft can just be accommodated by the Atlas V 511, or by the Delta IV 4240-12 with some launch mass margin.

The mission itinerary is summarized in table 11 and a plot showing the mission trajectories (ecliptic plane projection) is presented in figure 15.

Table 11. Preliminary mission design to visit four human-accessible NEAs.

Starting Location	Destination	Departure Date	Flight Time (days)	Stay Time (days)	ΔV_{DEP} (m/s)	ΔV_{ARR} (m/s)
Earth	1991 VG	12/11/2017	328	204	$(C_3 = 0.790 \text{ km}^2/\text{s}^2)$	152
1991 VG	2008 EA ₉	05/27/2019	300	322	1680	1453
2008 EA ₉	2007 UN ₁₂	02/07/2021	222	98	951	874
2007 UN ₁₂	2001 GP ₂	12/24/2021	132	-	613	727

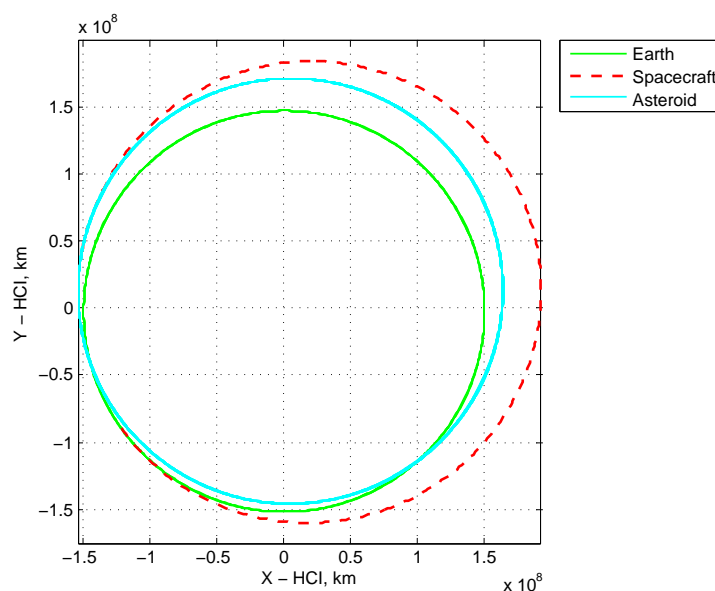


Figure 15. Trajectories for a robotic science tour of four human-accessible NEAs launching in 2017.

The preliminary multi-NEA mission designs presented herein were focused on attempting to fit in one of the more affordable launch vehicles. However, single-launch mission designs that visit at least several more NEAs (possibly a substantially larger number of NEAs) than the mission designs presented herein are possible if the mission budget could afford one of the larger Atlas V series launch vehicles, such as the 521, 531, 541, or 551, or one of the two largest Delta IV series launch vehicles, which are the 4450-14 and the 4050H-19. Furthermore, experience has shown that the number of NEA visits achieved with a single launch will also improve as the diversity of the candidate target NEA pool is increased; the candidate pools used for the preliminary analysis presented herein were purposely made small for convenience.

Finally, it must be noted that during the previously referenced study that utilized the Series Method to study the re-fueling of geostationary satellites, a discovery was made whereby a simple additional processing step can be added to the Series Method algorithm to achieve substantially improved performance (in terms of minimizing the total propellant required to visit a given number of targets) in most cases, but there was not enough time to apply that improvement to the preliminary study of multi-NEA precursor missions presented herein. We plan to apply that improvement in future work, and we expect that doing so will allow us to produce multi-NEA trajectory designs that are substantially improved over those presented herein.

IV. Conclusion

NASA may choose to send humans on an unprecedented interplanetary journey to a Near-Earth Asteroid in the year 2025, and to inform this effort we have developed a robust, flexible, and highly capable algorithm that can identify NEAs accessible for human exploration. As of February 19th, 2010, 59 accessible NEAs have been found, along with 10 marginally inaccessible NEAs that could be reached if the notional heavy-lift launch architecture was capable of launching less than 10% more mass into the outbound trajectory. A total of 319 NEAs have been discovered since February 19th, 2010 and will be processed as soon as this project resumes. The algorithm is fully parametrized and largely automated, even in its current relatively early state of development. The processing software can easily be fully automated and the algorithm is computationally efficient enough that the search for accessible NEAs can readily keep pace with the increasing NEA discovery rate using only modest computing resources, thereby enabling a comprehensive ongoing survey of NEAs that may be accessible for human exploration.

A great deal of work was performed in a relatively short amount of time to develop this capability, and along the way we have identified a number of important future work topics.

IV.A. Future Work

IV.A.1. Full Automation

Perhaps the most important item for future work is the full end-to-end automation of the accessibility analysis processing. The algorithm is already fully parametrized and runs in an automated fashion (though it must be initiated manually), and all of the pre- and post-processing steps are manually executed with self-contained individual programs. It would be relatively straightforward to chain everything together and have one master control computer automatically access newly discovered asteroid ephemeris files as they become available, process them, post-process the results, and update a living database of NEA accessibility results consisting of the accessible asteroids, the marginally inaccessible asteroids, trajectory solutions for the most attractive NEAs, accessibility space plots, robotic precursor mission design results (including near-optimal multi-destination precursor mission designs), and a variety of other automatically generated data products that we might design to compliment the existing array of data tables and plots.

IV.A.2. Addressing Ephemeris Uncertainties

Asteroid orbits are of course only known to within a certain precision, and the orbit determination results for a given asteroid may change as new observations are made or pre-discovery observations are obtained. It would be straightforward to add an automated processing step whereby the JPL asteroid ephemerides would be downloaded at regular intervals and compared to the most recent set of downloaded ephemeris files. Any NEA whose new ephemeris file showed a delta with respect to the previous ephemeris file would then be re-processed to determine if its accessibility profile is changed as a result of the new ephemeris; the accessible asteroid database would then be updated accordingly.

Additionally, it would be interesting to derive the mathematical relationships between the covariance of the asteroid ephemerides and the accessibility space. These relationships would allow the certainty of each asteroid's accessibility to be quantified as part of the accessibility analysis algorithm. Developing such statistics largely requires analyzing and determining the sensitivity of trajectory design results to NEA orbit determination uncertainty.

IV.A.3. Processing Speed Enhancement

After completing the accessibility data processing presented herein, we began profiling our Lambert trajectory solver algorithm and experimenting with different types of Lambert solvers in conjunction with a separate project. We discovered a much more computationally efficient Lambert solver that produces identical results to those generated by our current solver. This new Lambert algorithm is faster than the current algorithm by a factor of 3 or more, and using it in lieu of our current solver would accordingly increase the accessibility processing speed tremendously. Processing speed could be further increased by adding a bracketing method to the current bisection method table search that we use to index into the ephemeris files. Finally, processing speed will clearly increase if the fastest computers available are utilized. We have not yet collected statistics that would allow us to quantify the projected increase in processing speed as computing power increases.

IV.A.4. Website Development

If the accessibility processing is fully automated, it would make sense to have all of the results and data products organized on a central server and then create a website interface for browsing and manipulating the results. This would facilitate collaboration between the various NASA centers, JPL, and those engaged in NEA survey/characterization research. The website might consequently influence observation priorities at facilities on the ground and in space. Appropriate access controls could easily be put in place, and all users could have the option of subscribing to an automated email system that would transmit notifications as newly discovered NEAs are processed, new NEA observations are processed, and new accessibility results are obtained. The web interface could be made powerful enough to permit easy browsing of all the accessibility data sets, and users could issue commands through the website to have specific trajectory plots, accessibility space plots and data tables generated for display within the web interface and/or for local download^x. Additionally, a wiki site could be built for documentation of all software and algorithms.

The website could also serve as a powerful public relations tool with which to communicate the exciting possibilities of NEA missions and educate the general public. It might even be possible to greatly expand the available computer processing power by extending the current processing automation to allow any user to contribute some of their computer's CPU time in the same manner as the SETI@Home project.

IV.A.5. Vehicle Trade Studies

The complete parametrization of the accessibility analysis algorithm allows a variety of trade studies on vehicle performance parameters to be performed, the results of which may inform the design and use of future heavy-lift launch vehicles and crew vehicles for NEA missions. The goal would be to design an illustrative array of vehicle performance parameter combinations and execute the accessibility analysis algorithm on the entire NEA population for all vehicle parameter combinations. Key parameters to vary include: crew vehicle dry mass, crew vehicle thruster specific impulse, launch vehicle available payload mass as a function of C_3 , and maximum allowable Earth atmosphere re-entry velocity. We can study the impacts of the various combinations of these parameters on the overall NEA accessibility space. Additionally, our algorithms will be modified to permit the modeling of other architecture techniques, such as multiple heavy-lift launch vehicles or pre-emplaced consumable or shielding mass at the NEA destination, so that trade studies can be performed that include these options.

In parallel to this effort we would also like to perform more rigorous study of the crew vehicle requirements for a NEA mission, perhaps including a habitat module with the crew vehicle, which would of course increase the effective crew vehicle dry mass but would also theoretically extend the amount of time that the crew can safely spend in transit or loitering with an NEA by virtue of additional radiation shielding and living space. However, all of the relevant factors for interplanetary human spaceflight would have to be considered, and we would ultimately like to construct detailed parametric models for the crew vehicle dry mass as a function of mission parameters; utilizing this model would provide a more accurate accessibility assessment.

IV.A.6. Accounting for Earth Departure and Return Asymptote Declination Angles

We would like to develop a means of algorithmically accounting for the impact of Earth departure asymptote declination angle on launch vehicle performance. In that case, the available launch mass from the launch vehicle would be a function of both C_3 and the Earth departure asymptote declination angle. Additionally, we would like to develop a means of algorithmically determining the impact of Earth return asymptote declination angle on mission performance and thereby incorporate it appropriately into the accessibility analysis algorithm.

IV.A.7. Lunar Swingby

Performing a lunar swingby for a small gravity assist could improve the performance of the crew vehicle and augment the NEA accessibility space accordingly, making some of the marginally inaccessible asteroids become accessible, or allowing currently accessible asteroids to be reached slightly faster or with somewhat more desirable launch dates. While lunar gravity assist is likely a second-order effect and would depend strongly on the lunar ephemeris, it is worth investigating and so we currently have an Emergent Space

^xFollowing through on the theme of supporting NEA characterization observers with this site, a product or tool estimating apparent magnitude, solar elongation, and range from a geocentric location might be appropriate

Technologies, Inc. summer intern performing an analysis of how the Earth-Moon system dynamics might aid round-trip missions to NEAs^y.

IV.A.8. Visualization Enhancements

Apart from continuing to develop and refine post-processing tools for creating instructive static plots of the NEA mission trajectory features and accessibility spaces, it is possible to create videos and animations showing the mission trajectory sequences with high-quality graphics using free open-source software such as Celestia. Celestia is fully scriptable and ingests simply formatted ASCII trajectory data files; modifying the accessibility processing software to automatically output trajectory sets in the Celestia format, along with script files, would be a straightforward matter and would facilitate the creation of mission animations that would serve as excellent tools by which to communicate exciting results to management and the general public. An excellent example of such an animation has already been created via video capture from Celestia's simulation of the outbound trajectory to 1999 AO₁₀ launched in September 2025^z.

IV.A.9. Asteroid Rendezvous and Proximity Operations

Some preliminary studies into terminal rendezvous and proximity operations maneuvers in the vicinity of NEAs have been performed and we would like to continue these studies, drawing upon our own experience in this area and incorporating recent work on this topic performed by others. Simulating and studying spacecraft guidance, navigation, and control relative to a NEA will be important to our holistic mission design efforts and will be necessary to inform more rigorous designs of the crew vehicle.

Acknowledgments

This work was funded by the NASA Goddard Space Flight Center.

References

- ¹Nuth, J. A., "How were the comets made?" *American Scientist*, Vol. 89, pp. 230–237.
- ²Rohde, R. A. and Muller, R. A., "Cycles in fossil diversity," *Letters to Nature*, Vol. 434, 2005, pp. 208–210.
- ³Alvarez, L., Alvarez, W., Asaro, F., and Michel, H., "Extra-Terrestrial Cause for the Cretaceous–Tertiary Extinction," *Science*, Vol. 208, 1980, pp. 1095–1108.
- ⁴Barbee, B. W. and Nuth, J. A., "Asteroid Impact Threats: Advancements in Asteroid Science to Enable Rapid and Effective Deflection Missions," *Journal of Cosmology*, Vol. 2, 2009, pp. 386–410, <http://journalofcosmology.com/Extinction109.html>.
- ⁵Adamo, D. R., Giorgini, J. D., Abell, P. A., and Landis, R. R., "Asteroid Destinations Accessible For Human Exploration: A Preliminary Survey In Mid-2009," *AIAA Journal of Spacecraft and Rockets*, 2010, To Be Published.
- ⁶Sumrall, J. P., "Ares V Overview," Ares V Solar System Science Workshop, April 2008, <http://event.arc.nasa.gov/aresv-sss/home/ppt/AresV-sss/SAT/am/4Sumrall/7567AresVSolarSysWorkshop.pdf>.
- ⁷"NASA's Exploration Systems Architecture Study Final Report," Tech. Rep. NASA/TM-2005-214062, NASA, November 2005, <http://www.sti.nasa.gov>.
- ⁸"Human Exploration of Mars Design Reference Architecture 5.0," Tech. Rep. NASA-SP-2009-566, NASA, July 2009, http://www.nasa.gov/pdf/373665main_NASA-SP-2009-566.pdf.
- ⁹Hill, P. and Peterson, C., *Mechanics and Thermodynamics of Propulsion*, Addison-Wesley, 2nd ed., 1992, pp. 570–572.
- ¹⁰Farquhar, R. W., Dunham, D. W., Guo, Y., and McAdams, J. V., "Utilization of libration points for human exploration in the Sun-Earth-Moon system and beyond," *Acta Astronautica*, Vol. 55, August 2004, pp. 687–700.
- ¹¹Orloff, R. W. and Harland, D. M., *Apollo: The Definitive Sourcebook*, Springer-Praxis, 2006, p. 581.
- ¹²Press, W. H., Teukolsky, S. A., Vetterling, W. T., and Flannery, B. P., *Numerical Recipes in C: The Art of Scientific Computing*, Cambridge University Press, 2nd ed., 1992, pp. 117–119.
- ¹³Vallado, D. A., *Fundamentals of Astrodynamics and Applications*, Microcosm Press and Kluwer Academic Publishers, 2nd ed., 2001.
- ¹⁴Busch, M. W., Kulkarni, S. R., Ostro, S. J., Brisken, W., Benner, L. A. M., Nolan, M. C., Giorgini, J. D., Brozovic, M., and Magri, C., "Delay-Doppler and Radar-Interferometric Imaging of the Near-Earth Asteroid 2008 EV5," *AAS/Division for Planetary Sciences Meeting*, Vol. 41, Sept. 2009, p. 43.10.

^yA lunar gravity assist also suffers from another design downside in a human mission context. To ensure mission success, it's typically necessary to plan launch well in advance of the lunar encounter. This further extends mission duration compared to a more direct Earth departure trajectory

^zThis video is available at <http://www.youtube.com/watch?v=VYZg3ZXZ0qQ>. For a more immersive experience, select 720p HD resolution and full screen mode to view the video.

¹⁵Barbee, B. W., Davis, G. W., and Hur-Diaz, S., “Spacecraft Trajectory Design for Tours of Multiple Small Bodies,” *Advances in the Astronautical Sciences*, Vol. 135, Univelt, Inc., San Diego, CA, 2009, pp. 2169–2188, also AAS/AIAA Paper AAS 09-433, Astrodynamics Specialists Conference, Aug. 2009.

¹⁶Barbee, B. W., Carpenter, J. R., Heatwole, S., Markley, F. L., Moreau, M., Naasz, B. J., and Van Eepoel, J., “Guidance and Navigation for Rendezvous and Proximity Operations with a Non-Cooperative Spacecraft at Geosynchronous Orbit,” George H. Born Symposium, May 2010, Boulder, Colorado.

¹⁷Barbee, B. W., Alfano, S., Gold, K., Gaylor, D., and Piñon, E., “Mission Design for Multi-Object Orbital Debris Removal Tours,” George H. Born Symposium, May 2010, Boulder, Colorado.